

1-1-2019

Transcription factor binding site clusters identify target genes with similar tissue-wide expression and buffer against mutations.

Peter Rogan

The University of Western Ontario, progan@uwo.ca

Ruipeng Lu

The University of Western Ontario, rlu45@uwo.ca

Follow this and additional works at: <https://ir.lib.uwo.ca/biochempub>

Part of the [Biochemistry Commons](#), [Bioinformatics Commons](#), [Computational Biology Commons](#), and the [Genomics Commons](#)

Citation of this paper:

Lu R and Rogan PK. Transcription factor binding site clusters identify target genes with similar tissue-wide expression and buffer against mutations [version 2; peer review: 2 approved]. *F1000Research* 2019, 7:1933 (<https://doi.org/10.12688/f1000research.17363.2>)



RESEARCH ARTICLE

REVISED Transcription factor binding site clusters identify target genes with similar tissue-wide expression and buffer against mutations [version 2; peer review: 2 approved]

Ruipeng Lu¹, Peter K. Rogan 1-3

¹Computer Science, University of Western Ontario, London, Ontario, N6A 5B7, Canada

²Biochemistry, University of Western Ontario, London, Ontario, N6A 5C1, Canada

³Cytogenomics, London, Ontario, N5X 3X5, Canada

v2 **First published:** 14 Dec 2018, 7:1933 (<https://doi.org/10.12688/f1000research.17363.1>)
Latest published: 08 Apr 2019, 7:1933 (<https://doi.org/10.12688/f1000research.17363.2>)

Abstract

Background: The distribution and composition of *cis*-regulatory modules composed of transcription factor (TF) binding site (TFBS) clusters in promoters substantially determine gene expression patterns and TF targets. TF knockdown experiments have revealed that TF binding profiles and gene expression levels are correlated. We use TFBS features within accessible promoter intervals to predict genes with similar tissue-wide expression patterns and TF targets using Machine Learning (ML).

Methods: Bray-Curtis Similarity was used to identify genes with correlated expression patterns across 53 tissues. TF targets from knockdown experiments were also analyzed by this approach to set up the ML framework. TFBSs were selected within DNase I-accessible intervals of corresponding promoter sequences using information theory-based position weight matrices (iPWMs) for each TF. Features from information-dense clusters of TFBSs were input to ML classifiers which predict these gene targets along with their accuracy, specificity and sensitivity. Mutations in TFBSs were analyzed *in silico* to examine their impact on TFBS clustering and predict changes in gene regulation.

Results: The glucocorticoid receptor gene (*NR3C1*), whose regulation has been extensively studied, was selected to test this approach. *SLC25A32* and *TANK* exhibited the most similar expression patterns to *NR3C1*. A Decision Tree classifier exhibited the best performance in detecting such genes, based on Area Under the Receiver Operating Characteristic curve (ROC). TF target gene prediction was confirmed using siRNA knockdown, which was more accurate than CRISPR/CAS9 inactivation. TFBS mutation analyses revealed that accurate target gene prediction required at least 1 information-dense TFBS cluster.

Conclusions: ML based on TFBS information density, organization, and chromatin accessibility accurately identifies gene targets with comparable tissue-wide expression patterns. Multiple information-dense TFBS clusters in promoters appear to protect promoters from effects of deleterious binding site mutations in a single TFBS that would otherwise alter regulation of these genes.

Open Peer Review

Referee Status:

| | Invited Referees | |
|------------------|------------------|--------|
| | 1 | 2 |
| REVISED | | |
| version 2 | report | report |
| published | | |
| 08 Apr 2019 | | |
| version 1 | | |
| published | report | report |
| 14 Dec 2018 | | |

- 1 **Daphne Ezer** , The Alan Turing Institute for Data Science, UK
- 2 **Nicolae Radu Zabet** , University of Essex, UK

Any reports and responses or comments on the article can be found at the end of the article.

Keywords

Transcription factors, position-specific scoring matrices, chromatin, binding sites, gene expression profiles, Bray-Curtis similarity, mutation, machine learning, information theory

Corresponding author: Peter K. Rogan (progan@uwo.ca)

Author roles: **Lu R:** Conceptualization, Data Curation, Formal Analysis, Methodology, Resources, Software, Validation, Visualization, Writing – Original Draft Preparation, Writing – Review & Editing; **Rogan PK:** Conceptualization, Formal Analysis, Funding Acquisition, Methodology, Project Administration, Supervision, Writing – Original Draft Preparation, Writing – Review & Editing

Competing interests: PKR is the inventor of US Patent 5,867,402 and other patents pending, which apply iPWMs to the prediction and validation of mutations. He cofounded Cytognomix, Inc., which is developing software based on this technology for complete genome or exome mutation analysis.

Grant information: Natural Sciences and Engineering Research Council of Canada Discovery Grant [RGPIN-2015-06290]; Canada Foundation for Innovation; Canada Research Chairs. RL was supported by a fellowship from the Southern Ontario Smart Computing Innovation Platform, the Ontario Centres of Excellence Talent Edge program and Cytognomix Inc. Compute Canada and Shared Hierarchical Academic Research Computing Network (SHARCNET) provided high performance computing and storage facilities. Funding for open access charge: University of Western Ontario and the Natural Sciences and Engineering Research Council.

The funders had no role in study design, data collection and analysis, decision to publish, or preparation of the manuscript.

Copyright: © 2019 Lu R and Rogan PK. This is an open access article distributed under the terms of the [Creative Commons Attribution Licence](#), which permits unrestricted use, distribution, and reproduction in any medium, provided the original work is properly cited.

How to cite this article: Lu R and Rogan PK. **Transcription factor binding site clusters identify target genes with similar tissue-wide expression and buffer against mutations [version 2; peer review: 2 approved]** F1000Research 2019, 7:1933 (<https://doi.org/10.12688/f1000research.17363.2>)

First published: 14 Dec 2018, 7:1933 (<https://doi.org/10.12688/f1000research.17363.1>)

REVISED Amendments from Version 1

The manuscript has been extensively edited to improve clarity of the presentation. Sentence lengths were reduced. Duplicate terms and text were eliminated. The titles of the subsections of Results were revised to indicate the primary conclusions. Two paragraphs were moved to the Supplementary Methods. The revised manuscript is shortened by 400 words and approximately 2 pages.

We addressed the impact of covariance between expression levels of developmentally related tissues from the same organ, by sequentially removing 12 of 13 brain tissues from the GTEx dataset prior to recomputing the Bray-Curtis Similarity index. We found multiple covarying brain tissue expression values to not significantly influence the set of most similar genes seen with all 53 tissues in this analysis.

For the Decision Tree classifiers predicting transcription factor target genes, Gini importance values were computed to assess the relative contribution of the six ML features to their predictive power. For the CRISPR-perturbed TFs in the K562 cell line, clustering Features 1-3, particularly the TFBS cluster information densities (Feature 3), were most important. The TFBS-level Feature 5 comprising the distribution of strong binding sites accounts for the largest contribution to classifier performance for the 11 siRNA-perturbed TFs in the GM19238 cell line.

Additional file 1 now contains text from v1 of the manuscript as requested by a reviewer. Additional file 5 now contains the Gini scores for the machine learning features and the accuracy value of each individual round of 10-fold cross validation.

We now cite:

- Zabet & Adryan (2015)-indicating properties of TF molecules that contributed to genome-wide binding profiles.
- Ma *et al.* (2018)-describing spatially colocalized cis-clusters of TFs and how these groups of TF constitute tissue specific regulatory subnetworks.
- Applications of Bray-Curtis Similarity in genomics (<https://precision.fda.gov/challenges/3/view/results>), geosocial networks (Chen *et al.*, 2014; Chen *et al.*, 2014), and ecology (Ricotta *et al.*, 2017).

See referee reports

Introduction

The distinctive organization and combination of TFBSs and regulatory modules in promoters dictates specific expression patterns within a set of genes¹. Clustering of multiple adjacent binding sites for the same TF (homotypic clusters) and for different TFs (heterotypic clusters) defines *cis*-regulatory modules (CRMs) in human gene promoters. Experimental studies have shown that these clusters can reinforce (and in some instances, amplify) the impact of individual TFBSs on gene expression through increasing binding affinities, facilitated diffusion mechanisms and funnel effects². Because tissue-specific TF-TF interactions in TFBS clusters are prevalent, these features can assist in identifying correct target genes by altering binding specificities of individual TFs³. Previously, we derived iPWMs from ChIP-seq data that can accurately detect TFBSs and quantify their strengths by determining the associated R_i values (Rate of Shannon information transmission for an individual sequence⁴). $R_{sequence}$ (the area under the sequence logo) is the average of R_i values of all binding

site sequences and represents the average binding strength of the TF³. Neighboring, likely coregulatory TFBSs were identified by information density-based clustering (IDBC), which takes into account both the spatial organization (i.e. intersite distances) and information density (i.e. R_i values) of TFBSs⁵.

TF binding profiles, either derived from *in vivo* ChIP-seq peaks⁶⁻⁸ or computationally detected binding sites and CRMs⁹, have been shown to be predictive of absolute gene expression levels using a variety of tissue-specific ML classifiers and regression models. Because signal strengths of ChIP-seq peaks are not strictly proportional to strengths of the contained strongest TFBSs and are instead controlled by TFBS counts^{3,10}, representing TF binding strengths by ChIP-seq signals may not be appropriate; nevertheless, both achieved similar accuracy¹¹. CRMs have been formed by combining two or three adjacent TFBSs⁹, which is inflexible, as it arbitrarily limits the number of binding sites contained in a module, and does not consider differences between information densities of different CRMs. Chromatin structure (e.g. histone modification (HM) and DNase I hypersensitive sites (DHSs)) were also found to be statistically redundant with TF binding in explaining tissue-specific mRNA transcript abundance at a genome-wide level^{7,8,12,13}, which was attributed to the heterogeneous distribution of HMs across chromatin domains⁸. Combining these two types of data explained the largest fraction of variance in gene expression levels in multiple cell lines^{7,8}, suggesting that either contributes unique information to gene expression that cannot be compensated for by the other.

Previous studies have shown that a small subset of target genes bound by TFs were differentially expressed (DE) in the GM19238 cell line, upon knockdown with small interfering RNAs (siRNAs)¹⁴. TFBS counts were defined as the number of ChIP-seq peaks overlapping the promoter, with the caveat that the number and strengths of the TFBSs in each peak were not known¹⁵. Correlation between total TFBS counts and gene expression levels across 10 different cell lines was more predictive of which were DE than by setting a minimum threshold count of TFBSs¹⁵. This has also been addressed by perturbing gene expression with CAS9-directed clustered regularly interspaced short palindromic repeats (CRISPR) of 10 different TF genes in K562 cells¹⁶. The regulatory effects of each TF were dissected by single cell RNA sequencing with a regularized linear computational model¹⁶. This revealed DE targets and new functions of individual TFs, some of which were likely regulated through direct interactions at TFBSs in their corresponding promoters. ML classifiers have also been applied to predict targets of a single TF using features extracted from *n*-grams derived from consensus binding sequences¹⁷, or from TFBSs and homotypic binding site clusters⁵.

We investigated whether the predicted TFBS strengths, distribution and CRM composition in promoters substantially determines gene expression profiles of direct TF targets. A general ML framework was developed by combining information theory-based TF binding profiles with DHSs. The approach predicts which genes have similar tissue-wide expression profiles, and conversely, DE direct TF targets. Upon selecting DHSs to define accessible

promoter intervals, ML features that captured the spatial distribution and information theory-based TFBS compositions of CRMs were extracted from IDBC clusters. The intent of this framework was to provide insight into the transcriptional program of genes with similar profiles by dissecting shared properties of their *cis*-regulatory element organization, without imposing strict constraints on the strengths and distributions of TFBSs. We first identify genes with comparable tissue-wide expression profiles by application of Bray-Curtis similarity¹⁸. Using transcriptome data generated by CRISPR¹⁶ and siRNA-based¹⁴ TF knockdowns, we predicted DE target genes with promoters that contain ChIP-seq peaks for these same TFs.

Methods

To identify genes with similar tissue-wide expression patterns, we formally define tissue-wide gene expression profiles and pairwise similarity measures between profiles of different genes. A general ML framework relates features extracted from the organization of TFBSs in these genes to their tissue-wide expression patterns. Since protein-coding (PC) sequences represent the most widely studied and best understood component of the human genome¹⁹, positives and negatives for deriving ML classifiers of predicted DE direct TF target genes encoding proteins (TF targets, below) were obtained from CRISPR- and siRNA-generated knockdown data.

Similarity between GTEx tissue-wide expression profiles of genes

We used data from the Genotype-Tissue Expression (GTEx, version 6p) project which measured expression levels for each gene in 53 tissues, in different numbers of individuals (5 to 564). For each tissue population, the median expression value is given in RPKM (Reads Per Kilobase of transcript per Million mapped reads) for each gene²⁰. Data are available on [Zenodo](#)²¹. To capture the tissue-wide overall expression pattern of a gene instead of within a single tissue, the tissue-wide expression profile of a gene was defined as its median RPKM across GTEx tissues, which is described by a 53-element vector (Equation 1). Note that different isoforms whose expression patterns may significantly differ from each other cannot be distinguished by this approach.

$$EP^A = [MEV_1^A, MEV_2^A, \dots, MEV_{53}^A] \text{ (in RPKM)} \quad (1)$$

where EP^A is the tissue-wide expression profile of Gene A, MEV_1^A is the median expression value of Gene A in Tissue 1, MEV_2^A is the median expression value of Gene A in Tissue 2, etc.

To discover other genes whose tissue-wide expression profiles are similar to a given gene, we computed the Bray-Curtis Similarity (Equation 2) between the tissue-wide expression profiles of all gene pairs. Relative to other similarity measures (Table 1, Additional file 1²²), this function exhibits desirable properties, including: 1) being bounded between 0 and 1, 2) achieving maximal similarity of 1, if and only if two vectors are identical, and 3) larger values having a larger impact on the resultant similarity value.

$$sim_{Bray-Curtis}(EP^A, EP^B) = \begin{cases} 1, & \text{if } \sum_{i=1}^{53} MEV_i^A = \sum_{i=1}^{53} MEV_i^B = 0 \\ 1 - \frac{\sum_{i=1}^{53} |MEV_i^A - MEV_i^B|}{\sum_{i=1}^{53} (MEV_i^A + MEV_i^B)}, & \text{otherwise} \end{cases} \quad (2)$$

Prediction of genes with similar tissue-wide expression profiles

The framework for predicting whether the tissue-wide expression profile of a gene resembles a particular gene is indicated in Figure 1 (panels A and B). The genomic locations of all DHSs in 95 cell types from the ENCODE project[23; hg38 assembly] were filtered for known promoters²⁴; these sequences were then scanned for TFBSs using 94 iPWMs corresponding to the primary binding motifs for 82 TFs³. Data are available on [Zenodo](#)²¹. Heterotypic TFBS clusters were detected with the IDBC algorithm by specifying a minimum threshold of $0.1 * R_{sequence}$ for the R_i values of individual TFBS elements in potential clusters; this eliminated weak binding sites detected with iPWMs corresponding to false positive, non-functional TFBSs³.

The seven information density-related ML features (Additional file 1²²) derived from each TFBS cluster included: 1) The distance between this cluster and the transcription start site (TSS), 2) The length of this cluster, 3) The information content of this cluster (i.e. the sum of R_i values of all TFBSs in this cluster), 4) The number of binding sites of each TF within this cluster, 5) The number of strong binding sites ($R_i > R_{sequence}$) of each TF within this cluster, 6) The sum of R_i values of binding sites of each TF within this cluster, and 7) The sum of

Table 1. Comparison between metrics in measurement of similarity between GTEx tissue-wide expression profiles of genes.

| Similarity metric | Property 1†,‡ | Property 2† | Property 3† |
|------------------------------------|---------------|-------------|-------------|
| Bray-Curtis | √; [0,1] | √ | √ |
| Euclidean | √; (0,1] | √ | × |
| Cosine | √; [0,1] | × | √ |
| Pearson correlation ²⁵ | × | × | × |
| Spearman correlation ²⁶ | × | × | × |

†The symbols √ and ×, respectively, indicate that the similarity metric satisfies and does not satisfy the property. ‡The interval in each cell indicates the range in which the result computed by the similarity metric lies.

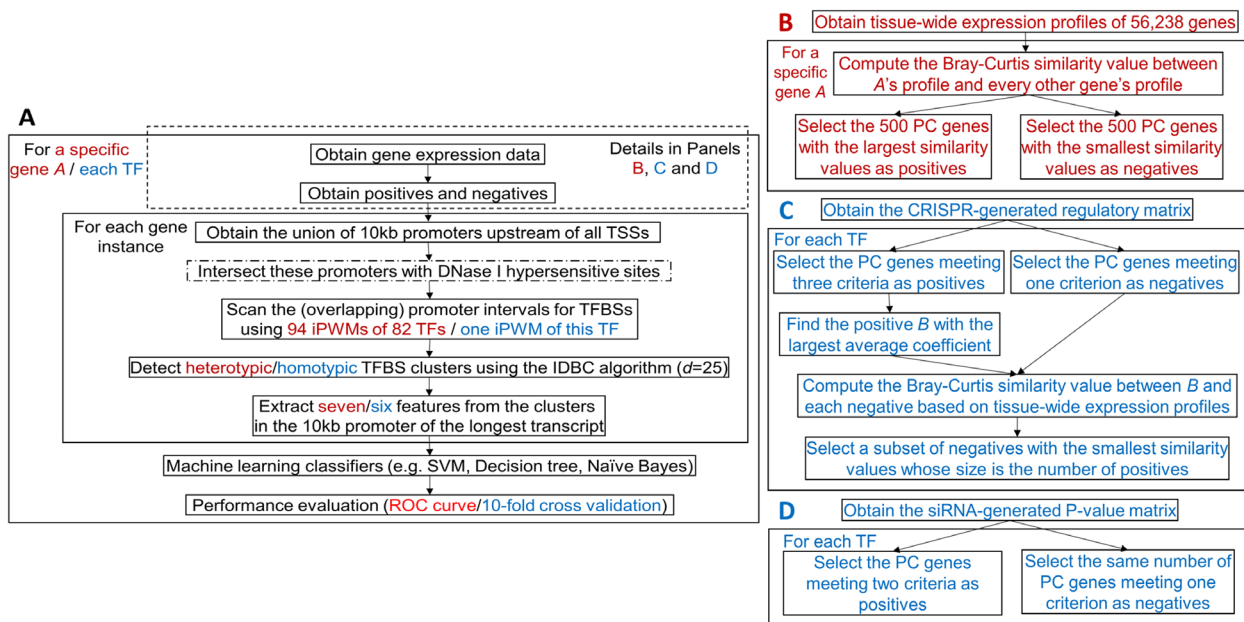


Figure 1. The general framework for predicting genes with similar tissue-wide expression profiles and TF targets. Red and blue contents are respectively specific to prediction of genes with similar tissue-wide expression profiles and prediction of TF targets. **(A)** An overview of the ML framework. The steps enclosed in the dashed rectangle vary across prediction of genes with similar tissue-wide expression profiles and TF targets. The step with a dash-dotted border that intersects promoters with DHSs is a variant of the primary approach. In the IDBC algorithm (Additional file 1²²), the parameter l is the minimum threshold on the total information contents of TFBS clusters. In prediction of genes with similar tissue-wide expression profiles, the minimum value was 939, which was the sum of mean information contents ($R_{sequence}$ values) of all 94 iPWMs; in prediction of direct targets, this value was the $R_{sequence}$ value of the single iPWM used to detect TFBSs. The parameter d is the radius of initial clusters in base pairs, whose value, 25, was determined empirically. The seven ML features derived from TFBS clusters are described in the Methods section. The performance of seven different classifiers was evaluated with ROC curves and 10-fold cross validation (Additional file 1²²). **(B)** Obtaining the positives and negatives for identifying genes with similar tissue-wide expression profiles to a given gene (Additional file 2²²). **(C)** Obtaining the positives and negatives for predicting target genes of seven TFs using the CRISPR-generated perturbation data in K562 cells (Additional file 3²²). **(D)** Obtaining the positives and negatives for predicting target genes of 11 TFs using the siRNA-generated knockdown data in GM19238 cells (Additional file 4²²).

R_i values of strong binding sites ($R_i > R_{sequence}$) of each TF within this cluster.

Each of the Features 1–3 was defined in a gene as a vector, whose size equalled the number of clusters in the gene promoter; each cluster was mapped to a single value in the vector. In Features 4–7, each cluster itself was mapped to a vector corresponding to binding sites for 82 TFs (Additional file 1²²). If two genes contained different numbers of clusters, the maximum number of clusters among all instances was determined, and null clusters were added to the 5' end of promoters with the smaller numbers of clusters; this enabled all genes to exhibit the same cluster counts. This allowed all genes to be used as training data for ML classifiers. Default parameter values for these classifiers were used to generate ROC curves with a built-in MATLAB function (Additional file 1²²).

Prediction of TF targets

Perturbed target gene expression after CRISPR-based mutation of TF genes. Dixit *et al.* performed CRISPR-based perturbation

experiments using multiple guide RNAs for each of ten TFs in K562 cells, resulting in a matrix of coefficients indicating the effect of each guide RNA on each of 22,046 genes¹⁶. Data are available on Zenodo²¹. The coefficient of a guide RNA is defined as the \log_{10} fold change in gene expression level¹⁶. We previously derived iPWMs for the primary binding motifs of 7 of the ten TFs (EGR1, ELF1, ELK1, ETS1, GABPA, IRF1, YY1)³. The framework for predicting TF targets (Figure 1A and 1C) was applied to these TFs. We defined a positive TF target gene in a cell line as :

- 1) The fold change in the expression level of this gene for each of the guide RNAs of the TF was consistently greater than (or is less than) 1, which eliminated genes exhibiting both increased and decreased expression levels for different guide RNAs, and increased the possibility that the gene was downregulated (or upregulated) by the TF (Additional file 1²²), and
- 2) The average fold change in the expression level of this gene for all guide RNAs of the TF was greater than the threshold ϵ (or is less than $1/\epsilon$), and

- 3) The promoter interval (10 kb) upstream of a TSS of this gene overlapped a ChIP-seq peak of the TF in the cell line.

If the coefficients for all guide RNAs of the TF for a gene were zero, the gene was defined as a negative (i.e. a non-target gene). As the threshold ϵ increases, the number of positives strictly decreases. As ϵ decreases, we have lower confidence that the positives were DE as a result of the TF perturbation. We balanced the number of positives obtained against our confidence that they were DE by evaluating different values of ϵ (i.e. 1.01, 1.05 and 1.1; Additional file 1²²). For each TF, all ENCODE ChIP-seq peak datasets from the K562 cell line were merged to determine positives. Data are available on [Zenodo](#)²¹. To avoid imbalanced datasets that significantly compromised the classifier performance²⁷, the Bray-Curtis function was applied to compute the similarity values in the tissue-wide expression profile between all negatives and the positive gene with the largest average coefficient, and then negatives with the smallest values were selected, resulting in the same number of positive and negative genes ([Figure 1C](#)).

Because TFs may exhibit tissue-specific sequence preferences due to different sets of target genes³, the K562 cell line-derived iPWMs of EGR1, ELK1, ELF1, GABPA, IRF1, YY1 were used to detect binding sites in DHS-intersected intervals; for ETS1, we used the only available iPWM from GM12878³. Six features (Features 1-5 and 7) were derived from each homotypic cluster (i.e. Feature 6 became identical to Feature 3, because only binding sites from a single TF were used) ([Figure 1A](#)). The results of 10 rounds of 10-fold cross validation were averaged to evaluate the accuracy of the classifier.

Target gene expression changes after siRNA-based knock-down of TFs. Significant changes in expression of target genes upon knockdown of 59 TFs in the GM19238 line were identified from the probability of differences in expression level (P-value) relative to the null hypothesis of no change¹⁴. Data are available on [Zenodo](#)²¹. DE genes with larger changes exhibited smaller P-values. The distribution of ChIP-seq peaks were considered to be evidence of TF binding to the promoters of these genes¹⁴. Among these 59 TFs, we have previously derived iPWMs exhibiting primary binding motifs for 11 (BATF, JUND, NFE2L1, PAX5, POU2F2, RELA, RXRA, SP1, TCF12, USF1, YY1)³. For this reason, transcription targets of these TFs were predicted in the GM19238 cell line ([Figure 1A, D](#)).

For ML training, we defined a positive (i.e. a target gene) for a TF, if the P-value of this gene was ≤ 0.01 , and the promoter interval up to 10 kb upstream of a TSS overlapped one or more ChIP-seq peaks of the TF in GM12878. Other genes with P-values > 0.01 exhibited insufficient support for being TF targets and were labeled as negatives.

The iPWMs from GM19238 were used to detect binding sites for all TFs except for RELA, RXRA and NFE2L1. The iPWM from the GM19099 line was used for RELA, and for RXRA and NFE2L1, the only available iPWMs were derived from HepG2 and K562 cells, respectively. The DHSs in GM19238

were first remapped to the hg38 assembly using [liftOver](#), prior to being intersected with known promoters²⁸. Data are available on [Zenodo](#)²¹. Although the knockdowns were performed in GM19238, GM12878 and GM19099 are also lymphoblastic cell lines, with GM19099 and GM19238 both being derived from the Yoruban population. For this analysis, the iPWMs derived in GM12878 and GM19099 were more appropriate sources of accessible TFBSs than those from HepG2 and K562, since GM12878 and GM19099 are more likely comparable to GM19238 than HepG2 and K562. ML results were evaluated by averaging cross validation, as described above.

Mutation analyses on promoters of TF targets

To understand the significance of individual binding sites on the regulatory state of TF targets, we evaluated the effects of sequence changes in TFBSs that altered the R_i values of these sites, the definition of TF clusters, and whether consequential IDBC-related changes impacted the prediction of TF target genes. For example, mutations were sequentially introduced into the strongest binding sites in TFBS clusters of the EGR1 target gene, *MCM7*, to determine the threshold for cluster formation and whether disappearing clusters disabled *MCM7* expression. For one target gene of each TF from the CRISPR-generated perturbation data, effects of naturally occurring TFBS variants present in [dbSNP](#)²⁹ were also evaluated to explore aspects of TFBS organization that enabled both clusters and promoter activity to be resilient to binding site mutations. This was done by analyzing whether the occurrence of individual or multiple single nucleotide polymorphisms (SNPs) lead to the loss of binding sites and the corresponding clusters, and resulted in changes in the predictions for these targets.

Results

The Bray-Curtis Function can accurately quantify the similarity between tissue-wide gene expression profiles

We computed the similarity values ([Equation 2](#)) between the tissue-wide expression profiles of the glucocorticoid receptor (*GR* or *NR3C1*) gene and all other 18,812 PC genes to find genes with related profiles. NR3C1 is an extensively characterized TF with many known direct target genes³⁰. As a constitutively expressed TF activated by glucocorticoid ligands, the protein mediates up-regulation of anti-inflammatory genes by binding as homodimers to glucocorticoid response elements. Transcription of proinflammatory genes is down-regulated by complexing with other activating TFs (e.g. NFKB and AP1), thereby eliminating their ability to bind and activate targets³⁰. NR3C1 can bind its own promoter forming an auto-regulatory loop, which also contains functional binding sites of 11 other TFs (e.g. SP1, YY1, IRF1, NFKB) whose iPWMs have been developed and/or mutual interactions have been described previously^{3,30}. The tissue-wide expression profile of NR3C1 comprises all different splicing and translational isoforms (*GR α -A*, *GR α -B*, *GR α -C*, *GR α -D*, *GR β* , *GR γ* , *GR δ*). However, the profile averages out tissue-specific preferences of some isoforms, for example, *GR α -C* isoforms are significantly higher in the pancreas and colon, whereas levels of *GR α -D* are highest in spleen and lungs³⁰. We found that *SLC25A32* and *TANK* have the greatest similarity in expression to *NR3C1* (0.880 and 0.877 respectively), based on their overall similar expression patterns across the 53 tissues ([Figure 2](#)).

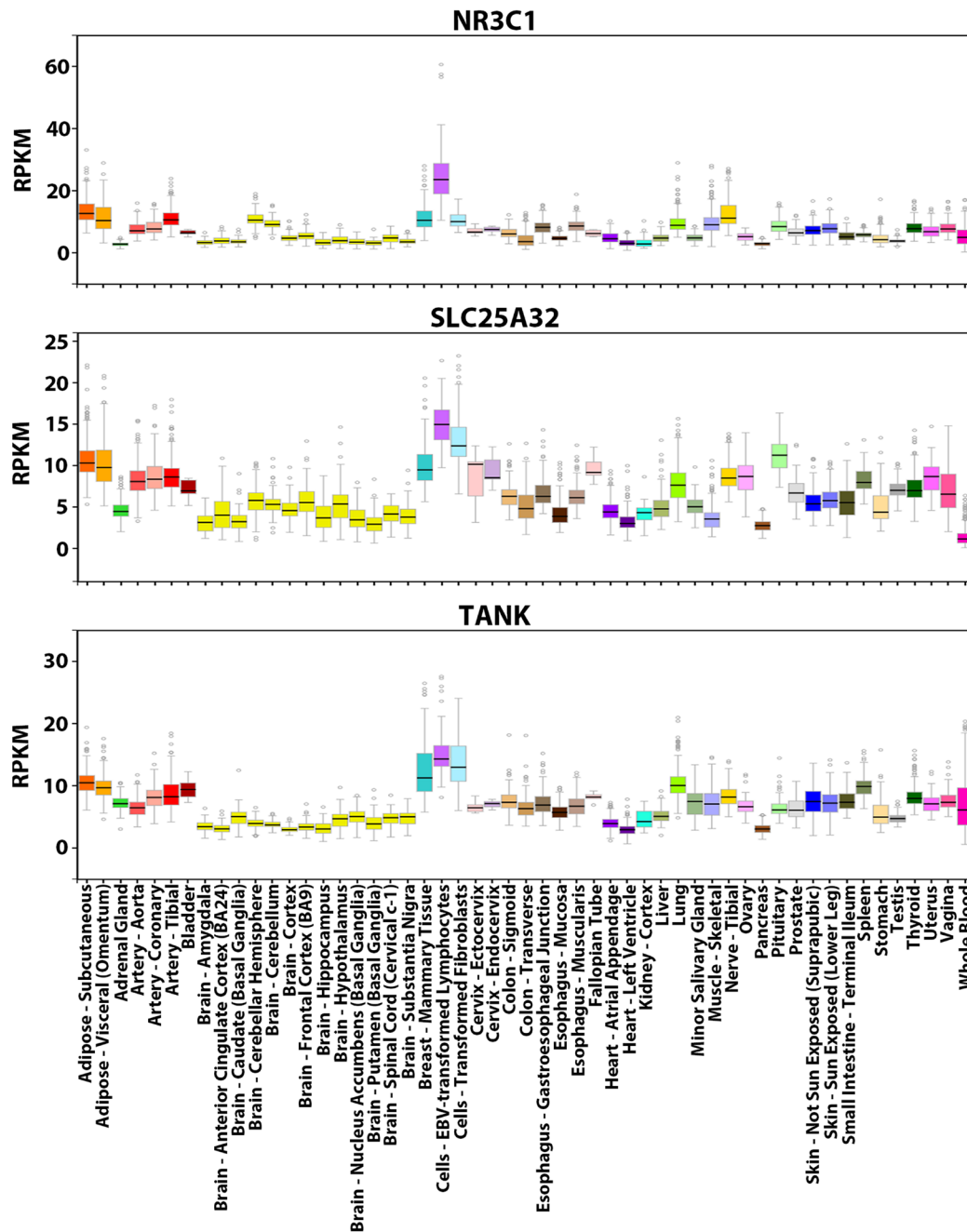


Figure 2. GTEx tissue-wide expression profiles of *NR3C1*, *SLC25A32* and *TANK*. Visualization of the expression values (in RPKM) of these genes across 53 tissues from GTEx. For each gene, the colored rectangle belonging to each tissue indicates the valid RPKM of all samples in the tissue, the black horizontal bar in the rectangle indicates the median RPKM, the hollow circles indicate the RPKM of the samples considered as outliers, and the grey vertical bar indicates the sampling error. A comparison of the panels shows that the overall expression patterns of the three genes across the 53 tissues resemble each other (e.g. all three genes exhibit the highest expression levels in lymphocytes and the lowest levels in brain tissues).

The Decision Tree classifier performed best in prediction of genes with similar tissue-wide expression profiles

Several ML classifiers (Naïve Bayes, Decision Tree (DT), Random Forest and Support Vector Machines (SVM) with four different kernels) were evaluated to determine how well TFBS-related

features could predict genes with tissue-wide expression profiles similar to *NR3C1*. Their performance were compared using ROC curves, for complete promoters or for accessible promoter sequences that were first intersected with DHSs (Figure 3). DT exhibited the largest AUC (area under the curve) under both

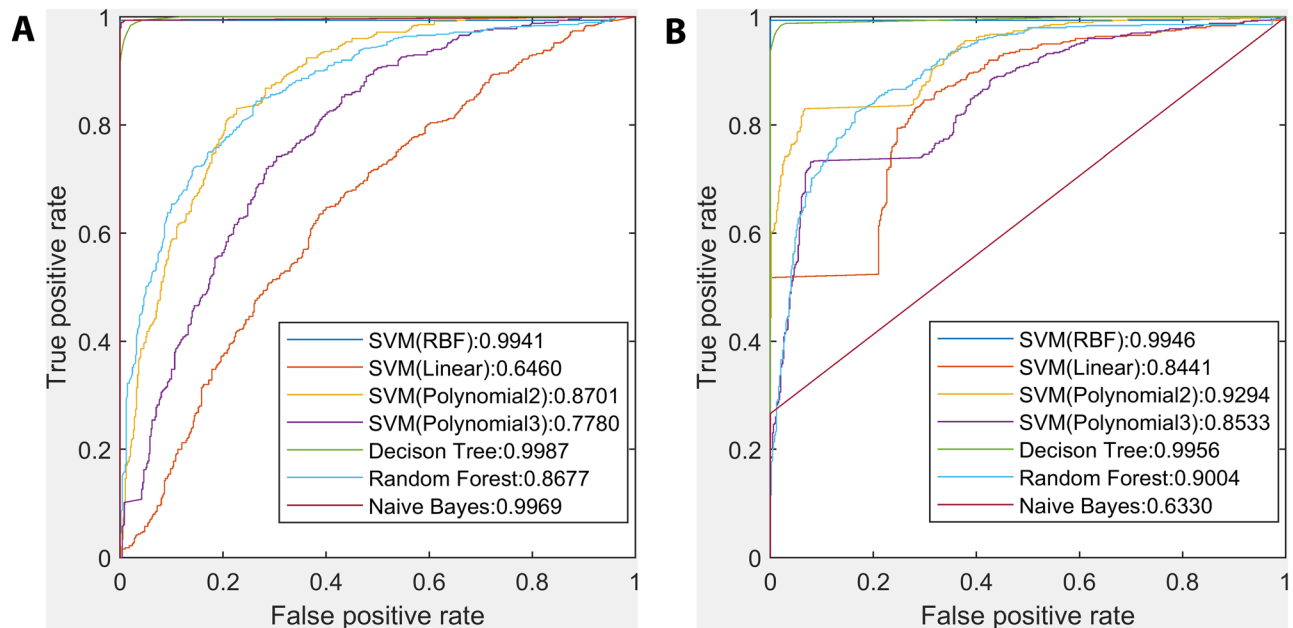


Figure 3. Comparison between the performance of different classifiers in prediction of genes with similar tissue-wide expression profiles to *NR3C1*. (A) ROC curves and AUC of seven classifiers without intersecting promoters with DHSs. (B) ROC curves and AUC of seven classifiers after intersecting promoters with DHSs. The Decision Tree classifier exhibited the largest AUC under both scenarios, and inclusion of DHS information significantly improved other classifiers' AUC except for Naïve Bayes.

scenarios, and was one of two most stable classifiers (i.e. $\Delta\text{AUC} < 0.01$), with the other being the SVM with RBF kernel. Consistent with previous findings^{10,31,32}, inclusion of DHS information significantly improved AUC values of the other classifiers with the exception of Naïve Bayes. In many instances, all TFBSs in a contiguous DHS interval formed a single binding site cluster.

The Decision Tree classifier was predictive of TF target genes

Based on its performance in distinguishing genes with *NR3C1*-like tissue-wide expression profiles, the DT classifier was used to predict TF targets respectively based on the CRISPR-¹⁶ and siRNA-generated¹⁴ perturbation data. Performance was assessed with 10 rounds of 10-fold cross validation (Tables 2 & Table 3). Gini importance values were also used to assess the relative contribution of the six ML features to the predictive power of the classifier (Additional file 5²²). For the CRISPR-perturbed TFs in the K562 cell line, clustering Features 1-3, particularly the TFBS cluster information densities (Feature 3), were most important. The TFBS-level Feature 5 comprising the distribution of strong binding sites accounts for the largest contribution to classifier performance for the 11 siRNA-perturbed TFs in the GM19238 cell line. To assess the value of all ML features in capturing the distribution and composition of CRMs in promoters, all but one (TFBS counts) were sequentially removed, and the impact on accuracy of the classifier was determined. In each instance,

classifier performance decreased, except for CRISPR-perturbed GABPA, IRF1 and YY1 upon inclusion of DHS information (Additional file 5²²).

The DT classifier predicted TF targets with greater sensitivity and specificity, after eliminating TFBSs in inaccessible promoter intervals in the CRISPR-generated knockdown data (Table 2). Specifically, predictions for EGR1, ELK1, ELF1, ETS1, GABPA, and IRF1 were more accurate than for YY1, which itself represses or activates a wide range of promoters by binding to sites overlapping the TSS (Table 2). Accordingly, perturbation results showed that YY1 has ~4-22 fold more PC targets in the K562 cell line than the other TFs ($\epsilon = 1.05$). Binding of YY1 more significantly impacts the expression levels of target genes. The ratio of the PC targets at $\epsilon = 1.1$ vs $\epsilon = 1.01$ was 0.334, which significantly exceeded those of other TFs in this study (0.017-0.082; Additional file 3²²). This is consistent with the extensive interactions of this factor with many other TF cofactors in K562 cells, and its central role in specifying erythroid-specific lineage development³.

We found that promoters of most TF targets contain accessible, likely functional binding sites that are significantly correlated with changes in gene expression levels. Despite a high accuracy of target recognition, sensitivity did not exceed specificity, except for IRF1 (Table 2), due to a relatively large number of false negative genes. Promoters of non-targets are either devoid of

Table 2. The Decision Tree classifier performance for predicting TF targets using the CRISPR-generated knockdown data.

| TF | Excluding DHS information† | | | Including DHS information† | | |
|-------|----------------------------|-------------|----------|----------------------------|-------------|----------|
| | Sensitivity | Specificity | Accuracy | Sensitivity | Specificity | Accuracy |
| EGR1 | 0.58 | 0.62 | 0.60 | 0.78 | 0.81 | 0.80 |
| ELF1 | 0.59 | 0.65 | 0.62 | 0.83 | 0.87 | 0.85 |
| ELK1 | 0.59 | 0.59 | 0.59 | 0.80 | 0.81 | 0.81 |
| ETS1 | 0.59 | 0.6 | 0.59 | 0.81 | 0.81 | 0.81 |
| GABPA | 0.55 | 0.57 | 0.56 | 0.72 | 0.75 | 0.74 |
| IRF1 | 0.54 | 0.55 | 0.54 | 0.76 | 0.64 | 0.70 |
| YY1 | 0.50 | 0.51 | 0.51 | 0.45 | 0.69 | 0.57 |

†The average performance of 10 rounds of 10-fold cross validation when setting ϵ to 1.05 is indicated. The accuracy of each individual round is indicated in Additional file 5²². The CRISPR-generated knockdown data were obtained from Dixit *et al.*¹⁶.

Table 3. The Decision Tree classifier performance for predicting TF targets using the siRNA-generated knockdown data.

| TF | Excluding DHS information† | | | Including DHS information† | | |
|--------|----------------------------|-------------|----------|----------------------------|-------------|----------|
| | Sensitivity | Specificity | Accuracy | Sensitivity | Specificity | Accuracy |
| BATF | 0.96 | 0.97 | 0.96 | 0.85 | 1 | 0.93 |
| JUND | 0.86 | 0.90 | 0.88 | 0.80 | 1 | 0.90 |
| NFE2L1 | 0.92 | 0.95 | 0.94 | 0.71 | 0.93 | 0.82 |
| PAX5 | 0.96 | 0.97 | 0.96 | 0.88 | 0.98 | 0.93 |
| POU2F2 | 0.97 | 0.97 | 0.97 | 0.89 | 0.99 | 0.94 |
| RELA | 0.95 | 0.96 | 0.96 | 0.83 | 0.97 | 0.90 |
| RXRA | 0.93 | 0.91 | 0.92 | 0.84 | 0.95 | 0.89 |
| SP1 | 0.98 | 0.98 | 0.98 | 0.89 | 0.99 | 0.94 |
| TCF12 | 0.98 | 0.98 | 0.98 | 0.86 | 0.99 | 0.93 |
| USF1 | 0.97 | 0.98 | 0.97 | 0.83 | 0.98 | 0.90 |
| YY1 | 1 | 1 | 1 | 0.55 | 0.99 | 0.77 |

†The average performance of 10 rounds of 10-fold cross validation is indicated. The accuracy of each individual round is shown in Additional file 5²². The siRNA-generated knockdown data were obtained from Cusanovich *et al.*¹³.

accessible binding sites, or these sites are non-functional. In these instances, the classifier was unable to distinguish between likely functional binding sites in targets and non-functional sites in non-targets. *In vivo* co-regulation mediated by interacting cofactors, which was excluded by the classifier, assisted in distinguishing these non-functional sites that do not significantly affect gene expression¹⁴.

As the minimum differential expression threshold ϵ increased, the accuracy of the classifier for all the TFs monotonically increased, as expected (Figure 4). In general, more significantly DE genes have been associated with a higher number of TFBSs in their promoters¹⁴. Thus, at greater ϵ , there are larger

differences in the values of ML features derived from TFBS clusters between direct targets and non-targets.

Some TF target genes also display similar tissue-wide expression profiles to the TFs, themselves

To determine how many TF targets have similar tissue-wide expression profiles, we intersected the set of targets with the set of 500 PC genes with the most similar tissue-wide expression profiles for each TF (Table 4, Additional file 6²³). For example, the B lymphocyte expression profiles of TFs PAX5 and POU2F2 are similar to their respective targets, *IL21R* and *CD86*. The intersected targets for YY1 include 21 and 7 nuclear mitochondrial genes (e.g. *MRPL9* and *MRPS10*, which are

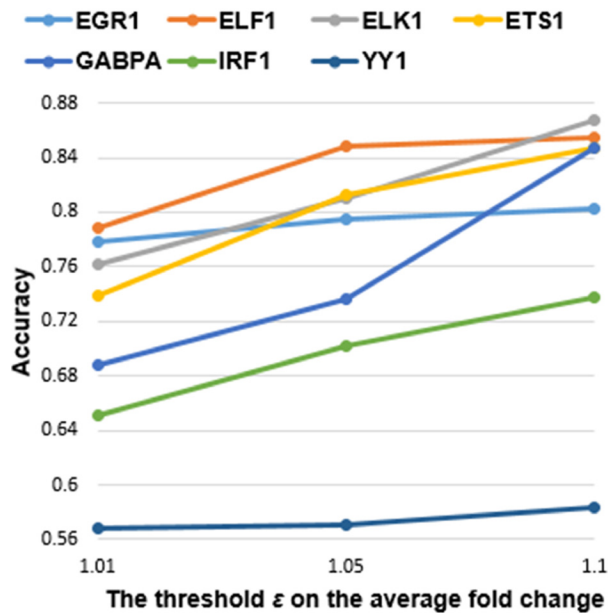


Figure 4. Accuracy of the Decision Tree classifier when using three different values for. Each accuracy value was averaged from 10 rounds of 10-fold cross validation. The minimum threshold ϵ of the average fold change in gene expression levels (for all guide RNAs) of the TF was determined for fold changes: 1.01, 1.05 and 1.1. The accuracy value of each individual round is indicated in Additional file 5²². As ϵ increased, accuracy for all seven TFs monotonically increased.

subunits of mitochondrial ribosomes), respectively, in the K562 and GM19238 cell lines³³. YY1 is known to upregulate a large number of mitochondrial genes by complexing with PGC-1 α in C2C12 cells³⁴, and genes involved in the mitochondrial respiratory chain in K562 cells¹⁶. Our results are consistent with the idea that YY1 may broadly regulate mitochondrial function within all 53 tissues, in addition to the erythrocyte, lymphocyte and skeletal muscle cell lines.

Between 0.4%–25% of genes with similar tissue-wide expression profiles to the TFs are actually their targets (Table 4). The majority are non-targets whose promoters contain non-functional binding sites that lack co-regulation by corresponding cofactors. For YY1 and EGR1, we contrasted the flanking cofactor binding site distributions and strengths in the promoters of the most similarly expressed target genes (YY1: *MRPL9*, *BAZ1B*; EGR1: *CANX*, *NPM1*) with non-target genes (YY1: *ADNP*, *RNF25*; EGR1: *GUCY2F*, *AWAT1*). In these target gene promoters, strong and intermediate TFBSs recognized by SP1, KLF1, CEBPB formed heterotypic clusters with adjacent YY1 sites. Additionally, TFBSs of SP1, KLF1, and NFY tended to be present adjacent to EGR1 binding sites (Additional file 7²²). These patterns contrasted with enrichment of CTCF and ETV6 binding sites in gene promoters of YY1 and EGR1 non-targets (Additional file 7²²). Previous studies have reported that KLF1 is essential for terminal erythroid differentiation and maturation³⁵. Direct physical interactions between YY1 and the constitutive activator SP1 synergistically induce transcription³⁶, through activating CEBPB which promotes differentiation and suppresses proliferation

Table 4. Intersection of TF targets and 500 protein-coding genes with the most similar tissue-wide expression profiles.

| TF | Cell line | Number of targets | Size of intersection | Targets among the most similar 10 genes§ |
|--------|-----------|-------------------|----------------------|---|
| EGR1 | K562 | 169 | 12 | None |
| ELF1 | | 78 | 5 | None |
| ELK1 | | 112 | 4 | <i>GNL1</i> (8 th) |
| ETS1 | | 267 | 15 | None |
| GABPA | | 513 | 25 | <i>TAF1</i> (1 st) |
| IRF1 | | 457 | 10 | None |
| YY1 | | 1752 | 127 | <i>MRPL9</i> (2 nd), <i>BAZ1B</i> (6 th), <i>ENY2</i> (7 th), <i>NUB1</i> (8 th), <i>USP1</i> (9 th), <i>HNRNPR</i> (10 th) |
| | GM19238 | 1040 | 61 | <i>MED4</i> (1 st), <i>SURF6</i> (3 rd), <i>BAZ1B</i> (6 th) |
| BATF | | 186 | 21 | None |
| JUND | | 44 | 2 | None |
| NFE2L1 | | 58 | 4 | None |
| RELA | | 247 | 13 | <i>HMG20B</i> (9 th) |
| RXRA | | 181 | 3 | None |
| SP1 | | 1595 | 81 | None |
| TCF12 | | 655 | 20 | None |
| USF1 | | 301 | 21 | None |
| PAX5 | | 918 | 86 | <i>IL21R</i> (8 th) |
| POU2F2 | | 532 | 26 | <i>CD86</i> (3 rd) |

§The rank of each target in the list of similar genes in the descending order of Bray-Curtis similarity values is shown in the brackets immediately following the target.

of K562 cells by binding the promoter of the *G-CSFR* gene encoding a hematopoietin receptor³⁷. EGR1 and SP1 synergistically cooperate at adjacent non-overlapping sites on *EGR1* promoter but compete for binding at overlapping sites³⁸, whereas occupied CTCF binding sites often function as an insulator blocking the effects of *cis*-acting elements and preventing gene activation by mediating long-range DNA loops to alter topological chromatin structure^{39,40}. ETV6, a member of the ETS family, is a transcriptional repressor required for bone marrow hematopoiesis and associated with leukemia development⁴¹.

Transcription factor binding site clusters buffer against expression changes from mutations in single sites

These results and previous studies indicate that the promoters of direct target genes contain multiple binding site clusters. We used our ML models of TFBS organization to investigate the effects of mutations in individual binding sites on the predicted expression of TF targets. We hypothesized that alternative TF clusters in the same promoter might stabilize and compensate for the loss of a mutated TF cluster, enabling mutated promoters to retain some capacity to regulate gene transcription upon TF binding. First, we introduced artificial variants into binding sites *in silico* in the promoter of the target gene *MCM7* of EGR1 and examined the effect on the output of the ML classifier (Figure 5). In the K562 line, *MCM7* is upregulated by EGR1. Knockdown of *MCM7* has an anti-proliferative and pro-apoptotic effect on K562 cells⁴² and the loss of EGR1 increases leukemia initiating cells⁴³, which suggests that EGR1 may act as a tumor suppressor in K562 cells through the *MCM7* pathway.

The strongest binding site (at position chr7:100103347[hg38], - strand, $R_i = 12.0$ bits) in the promoter was eliminated by a G->A mutation, resulting in the loss of Cluster 1 (Figure 5),

which consists of two sites (the other site at chr7:100103339, -, 4.3 bits). The other two clusters comprising weaker binding sites of intermediate strength (chr7:100102252, +, 7.0 bits; chr7:100102244, +, 1.3 bits; chr7:100101980, +, 8.9 bits; chr7:100101977, +, 2.2 bits; chr7:100101984, +, 1.9 bits) were still predicted to compensate for this mutation, so that the promoter maintains the capacity to induce *MCM7* expression (Figure 5). Adjacent sites within the same TFBS cluster, which may individually not have sufficient affinity to strongly bind TFs and activate transcription, are capable of stabilizing binding to adjacent sites². Weaker sites can direct TF molecules to strong sites and extend the duration of physical association, termed the funnel effect². Binding stabilization between adjacent sites and the funnel effect enable CRMs comprised of information-dense clusters to be robust to mutations in individual binding sites^{2,44}. In this example, Clusters 2 and 3 were also respectively removed by G->T and C->G mutations abolishing the strongest site in either cluster, altering the prediction of the classifier, that is, EGR1 is expected to fail to induce *MCM7* transcription (Figure 5). The remaining four sparse weak sites do not form a cluster and cannot completely supplant the disrupted strong sites.

We then examined the predicted impacts of natural SNPs on binding site strengths, clusters and predicted the regulatory state of the promoter for a direct target of each of the seven TFs from the CRISPR-generated perturbation data (Table 5). We found that a single SNP (e.g. rs996639427 of EGR1) could affect the strengths of multiple binding sites within a cluster (Table 5). Apart from SNPs that are predicted to abolish binding (Figure 5), leaky variants that are expected to merely weaken TF binding are also common (Table 5). Neither mutations that abolish TFBSs nor leaky SNPs in flanking weak binding sites would be expected to inactivate TFBS clusters

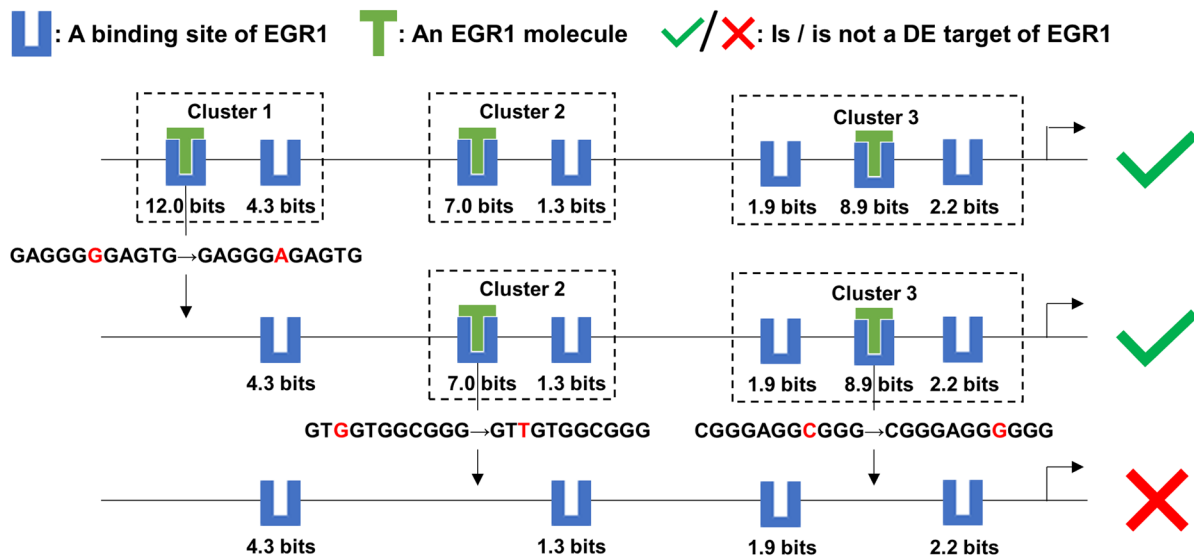


Figure 5. Mutation analyses on the target *MCM7* of EGR1. This figure depicts the effect of a mutation in each EGR1 binding site cluster of the *MCM7* promoter on the expression level of *MCM7*, which is a target of the TF EGR1. The strongest binding site in each cluster were abolished by a single nucleotide variant. Upon loss of all three clusters, only weak binding sites remained and EGR1 was predicted to no longer be able to effectively regulate *MCM7* expression. Multiple clusters in the promoters of TF targets confer robustness against mutations within individual binding sites that define these clusters.

Table 5. Mutation analyses on promoters of TF targets.

| TF | Target | Normal cluster | Normal binding site ^s | SNP ID ^s | Variant binding site ^s | Variant cluster [†] | Classifier output | | | | |
|--|---|-----------------------------------|---|---|---|------------------------------|----------------------|-----------|---|---|---|
| | | | | | | | Variant [†] | Wild-type | | | |
| EGR1 ($R_{sequence} = 12.2899$ bits) | EID2B | Cluster 1 of 2 | GAGGGGGCATC (chr19:39540296, -, 7.22 bits) | rs538610162 (chr19:39540296C>G) | C AGGGGGCATC (chr19:39540286, -, 4.84 bits) | Abolished | √ | × | √ | | |
| | | | | rs759233998 (chr19:39540294C>T) | GA AGGGGGCATC (chr19:39540286, -, 0.06 bit) | Abolished | √ | | | | |
| | | | | rs974735901 (chr19:39540288T>A) | GAGGGGG C TTC (chr19:39540286, -, 6.90 bits) | Cluster 1 of 2 | √ | | | | |
| | | | | rs978230260 (chr19:39540287A>T) | GAGGGGG CA AC (chr19:39540286, -, 5.31 bits) | Abolished | √ | | | | |
| | | Cluster 2 of 2 | GCGTGCGTGGG (chr19:39540162, +, 1.59 bits) | rs764734511 (chr19:39540162G>A) (chr19:39540162G>C) | AC GTGCGTGGG (chr19:39540162, +, -0.72 bit) | Cluster 2 of 2 | √ | | | × | √ |
| | | | | | CC GTGCGTGGG (chr19:39540162, +, -0.79 bit) | Cluster 2 of 2 | √ | | | | |
| | | | | rs996639427 (chr19:39540170G>C) | GCGTGCGT C GG (chr19:39540162, +, -5.21 bits) | Abolished | √ | | | | |
| | | | | | GCGT C GGCGCT (chr19:39540165, +, -0.85 bit) | | | | | | |
| | | | | rs1027751538 (chr19:39540174G>A) | GCGTGGG C ACT (chr19:39540166, +, 5.16 bits) | Abolished | √ | | | | |
| | | | | rs887888062 (chr19:39540176T>A) | <u>GCGTGGGCGCA</u> (chr19:39540166, +, 10.94 bits) | Cluster 2 of 2 | √ | | | | |
| ELF1 ($R_{sequence} = 11.2057$ bits) | HIST1H4H | Cluster 1 of 2 | GCGGAAGCGTG (chr6:26286540, +, 9.92 bits) | rs760968937 (chr6:26286547C>T) (chr6:26286547C>A) | <u>GCGGAAGTGTG</u> (chr6:26286540, +, 10.71 bits) | Cluster 1 of 2 | √ | × | √ | | |
| | | | | | GCGGAAG A GTG (chr6:26286540, +, 8.84 bits) | Cluster 1 of 2 | √ | | | | |
| | | | | rs1000196206 (chr6:26286542G>C) | G C GAAGCGTG (chr6:26286540, +, -6.26 bits) | Abolished | √ | | | | |
| | | | | rs144759258 (chr6:26286543G>A) | G C GAAGCGTG (chr6:26286540, +, -3.60 bits) | Abolished | √ | | | | |
| | | | | rs966435996 (chr6:26286544A>G) | GCGG G AGCGTG (chr6:26286540, +, 5.28 bits) | Abolished | √ | | | | |
| | | rs950986427 (chr6:26286548G>A) | GCGGAAG C ATG (chr6:26286540, +, 8.28 bits) | Cluster 1 of 2 | √ | | | | | | |
| | | Cluster 2 of 2 | CAGGAGATGCG (chr6:26286483, -, 6.98 bits) | rs373649904 (chr6:26286483G>A) | T AGGAGATGCG (chr6:26286473, -, 0.61 bit) | Abolished | √ | | | | |
| | | | | rs926919149 (chr6:26286480C>T) | CAG A AGATGCG (chr6:26286473, -, -6.53 bits) | Abolished | √ | | | | |
| | | | | rs751263172 (chr6:26286479T>G) | CAG G CGATGCG (chr6:26286473, -, 1.24 bits) | Abolished | √ | | | | |
| | | | | rs369076253 (chr6:26286473C>G) | CAGGAGATG C C (chr6:26286473, -, 6.92 bits) | Cluster 2 of 2 | √ | | | | |
| rs751263172 (chr6:1044474314C>T) | <u>CAGGAAATGCG</u> (chr6:26286473, -, 11.43 bits) | | | Cluster 2 of 2 | √ | | | | | | |

| TF | Target | Normal cluster | Normal binding site ^s | SNP ID ^s | Variant binding site ^s | Variant cluster [†] | Classifier output | | |
|---|---------|----------------|---|--|--|---|----------------------|-----------|---|
| | | | | | | | Variant [†] | Wild-type | |
| ELK1 ($R_{sequence} = 11.9041$ bits) | GOS2 | Cluster 1 of 2 | CAGGGAAGACC (chr1:209667969, -, 1.92 bits) | rs146048477 (chr1:209667961T>A) | CAGGGAAGTCC (chr1:209667959, -, 2.24 bits) | Cluster 1 of 2 | √ | √ | |
| | | | | rs887606802 (chr1:209667968T>C) | CGGGAAGACC (chr1:209667959, -, -3.35 bits) | Cluster 1 of 2 | √ | | |
| | | | | rs1021034916 (chr1:209667967C>T) | CAAGGAAGACC (chr1:209667959, -, -3.57 bits) | Cluster 1 of 2 | √ | | |
| | | | | rs941962117 (chr1:209667974A>G) | GAGGAGATGAG (chr1:209667969, +, 8.14 bits) | Abolished | √ | | |
| | | Cluster 2 of 2 | CTGGAAGAGCA (chr1:209673554, -, 5.91 bits) | rs896117033 (chr1:209673545G>A) | CTGGAAGAGTA (chr1:209673544, -, 3.95 bits) | Cluster 2 of 2 | √ | × | √ |
| | | | | rs971962577 (chr1:209673546C>T) | CTGGAAGAACA (chr1:209673544, -, 3.49 bits) | Cluster 2 of 2 | √ | | |
| | | | | rs1011969709 (chr1:209673554G>C) | GTGGAAGAGCA (chr1:209673544, -, 3.92 bits) | Abolished | √ | | |
| | | | | CCAGAAGTCAA (chr1:209673551, +, 7.44 bits) | rs1023312090 (chr1:209673561A>G) | CCAGAAGTCAG (chr1:209673551, +, 8.40 bits) | Cluster 2 of 2 | √ | √ |
| | | | | | | CCACAAGTCAA (chr1:209673551, +, -5.50 bits) | | | |
| | | | | | | | | | |
| ETS1 ($R_{sequence} = 10.0788$ bits) | TTC19 | Cluster 1 of 1 | GCAGGGAAAGG (chr17:16022293, +, 7.92 bits) | rs1022234223 (chr17:16022296G>C) | GCACGGAAAGG (chr17:16022293, +, -4.98 bits) | Abolished | × | × | |
| | | | | rs968299415 (chr17:16022301A>T) | GCAGGGAA TGG (chr17:16022293, +, 10.01 bits) | Cluster 1 of 1 | √ | √ | |
| GABPA ($R_{sequence} = 10.8567$ bits) | PLEKHB2 | Cluster 1 of 1 | ACAGGAAAGGG (chr2:131112770, +, 10.36 bits) | rs997328042 (chr2:131112771C>T) | ATAGGAAAGGG (chr2:131112770, +, -3.68 bits) | Abolished | × | | |
| | | | | rs1020720126 (chr2:131112773G>C) | ACACGAAAGGG (chr2:131112770, +, -4.16 bits) | Abolished | × | × | |
| | | | | rs185306857 (chr2:131112761C>A) | TATGGAAACTA (chr2:131112760, +, -2.86 bits) | Cluster 1 of 1 | √ | | |
| | | | TCTGGAAACTA (chr2:131112760, +, 1.53 bits) | rs772728699 (chr2:131112762T>A) | TCAGGAAACTA (chr2:131112760, +, 5.23 bits) | Cluster 1 of 1 | √ | | |
| | | | | rs965753671 (chr2:131112769T>C) | TCTGGAAACCA (chr2:131112760, +, 2.13 bits) | Cluster 1 of 1 | √ | | |
| | | | | | | | | | |

| TF | Target | Normal cluster | Normal binding site [§] | SNP ID [§] | Variant binding site [§] | Variant cluster [‡] | Classifier output | | |
|--|--------|----------------|--|--|--|------------------------------|----------------------|-----------|---|
| | | | | | | | Variant [†] | Wild-type | |
| IRF1 ($R_{sequence} = 13.5544$ bits) | SMIM13 | Cluster 1 of 1 | GAGAATGAAAGCA (chr6:11093663, +, 12.56 bits) | rs950528541 (chr6:11093663G>C) | C GAAATGAAAGCA (chr6:11093663, +, 8.97 bits) | Cluster 1 of 1 | √ | × | √ |
| | | | | rs886259573 (chr6:11093664A>G) | G GAAATGAAAGCA (chr6:11093663, +, 9.65 bits) | Cluster 1 of 1 | √ | | |
| | | | | rs982931728 (chr6:11093666A>G) | G AGATGAAAGCA (chr6:11093663, +, 8.09 bits) | Cluster 1 of 1 | √ | | |
| | | | | rs1020218811 (chr6:11093668T>G) | G AGAA G GAAAGCA (chr6:11093663, +, 9.36 bits) | Cluster 1 of 1 | √ | | |
| | | | | rs570723026 (chr6:11093672A>G) | G AGAATGA A GGCA (chr6:11093663, +, 8.01 bits) | Cluster 1 of 1 | √ | | |
| | | | | rs1004825794 (chr6:11093675A>C) (chr6:11093675A>T) | G AGAATGAAAG C C (chr6:11093663, +, 10.47 bits) | Cluster 1 of 1 | √ | | |
| | | | G AGAATGAAAG C A (chr6:11093663, +, 10.42 bits) | | Cluster 1 of 1 | √ | | | |
| | | | AAGACCAA A GGCA (chr6:11093641, +, 2.43 bits) | rs1030185383 (chr6:11093649A>C) | A AGACCAA C GGCA (chr6:11093641, +, -3.39 bits) | Cluster 1 of 1 | √ | | |
| | | | | rs5874306 (chr6:11093650delG) | A AGACCAA A GCAG (chr6:11093641, +, 0.90 bit) | Cluster 1 of 1 | √ | | |
| | | | | <u>rs558896490</u> (<u>chr6:11093643G>A</u>) | <u>AA</u> A ACCAA A GG C A (<u>chr6:11093641, +, 7.06 bits</u>) | Cluster 1 of 1 | √ | | |
| | | | | | | | | | |
| YY1 ($R_{sequence} = 12.8554$ bits) | CKLF | Cluster 1 of 1 | GCGGCCATCGGC (chr16:66549797, -, 10.06 bits) | rs865922947 (chr16:66549791G>A) | C CGGCCATCGGC (chr16:66549785, -, 6.80 bits) | Cluster 1 | √ | × | √ |
| | | | | rs946037930 (chr16:66549794C>A) | G CTGCCATCGGC (chr16:66549785, -, 8.02 bits) | Cluster 1 | √ | | |
| | | | | rs917218063 (chr16:66549793C>T) | G CG A CCATCGGC (chr16:66549785, -, 5.41 bits) | Abolished | × | | |
| | | | | rs928017336 (chr16:66549791G>A) | G CG G TCATCGGC (chr16:66549785, -, -3.62 bits) | Abolished | × | | |
| | | | GCCGCCCCCGTC (chr16:66549792, +, 1.34 bits) | | | | | | |

[§]All coordinates are based on the hg38 genome assembly. A bold italic letter in a binding site sequence indicates the base where a SNP occurs. For each normal and variant binding site sequence, the genome coordinate of its most 5'-end base and its R_i value are indicated. The negative R_i value of a variant binding site sequence implies this site is abolished. The SNPs strengthening binding sites and corresponding variant binding site sequences are underlined.

[‡]The impact on whether the occurrence of a single SNP resulted in the disappearance of the cluster containing it is shown; 'Abolished' indicates that the cluster is eliminated by the existence of the variant allele.

[†]After a single SNP occurred or multiple SNPs simultaneously occurred, the classifier produced a new prediction on whether the TF is still capable of significantly affecting gene expression via the variant promoter.

(e.g. rs1030185383 and rs5874306 of IRF1), whereas SNPs with large reductions in R_i values of strong sites are more likely to abolish clusters (e.g. rs865922947, rs946037930, rs917218063 and rs928017336 of YY1) (Table 5). Multiple TF clusters enable promoters to be resilient to the effects of these mutations; only

the complete inactivation of all clusters by concurrent effects of multiple SNPs within TFBSs would be capable of making a promoter to be unresponsive to TF binding (e.g. rs997328042, rs1020720126 and rs185306857 of GABPA) (Table 5). Conversely, a small number of SNPs capable of strengthening TF binding and

reinforcing the regulatory effect of the TF were also observed (e.g. rs887888062 of *EGR1* and rs751263172 of *ELF1*) (Table 5). In addition to deleterious mutations, potentially benign variants may also be found in promoters, consistent with the expectations of neutral theory⁴⁵.

Discussion

In this study, the Bray-Curtis similarity function was initially shown (for the *NR3C1* gene) to measure the relatedness of overall expression patterns between genes across a diverse set of tissues (Figure 2). A ML framework distinguished similar from dissimilar genes based on the distribution, strengths and compositions of TFBS clusters in accessible promoters, which can substantially account for the corresponding gene expression patterns (Figure 1 & Figure 3). Using gene expression knockdown data, the combinatorial use of TF binding profiles and chromatin accessibility was also demonstrated to be predictive of TF targets (Figure 4, Table 2 & Table 3). A binding site comparison confirmed that coregulatory cofactors can be used to distinguish between functional sites in targets and non-functional ones in non-targets. Furthermore, *in silico* mutation analyses on binding sites of targets suggested that the existence of both multiple TFBSs in a cluster and multiple information-dense clusters in the same promoter enables both the cluster and the promoter to be resilient to mutations in individual TFBSs (Figure 5, Table 5).

The DT classifier improved after intersecting promoters with DHSs in prediction of TF targets with the CRISPR-generated knockdown data (Table 2). This intersection eliminated noisy binding sites that are inaccessible to TF proteins in promoters^{10,31,32}; specifically, it widened discrepancies in feature vectors between positives and negatives. If the 10 kb promoter of a gene instance does not overlap DHSs, its feature vector will only consist of 0; the percentages of negatives whose promoters do not overlap DHSs considerably exceeded those of positives (Additional file 8²²), which led to an excess of negatives with feature vectors containing only 0 after intersection. This explains why these negatives are not DE targets of the TFs in the K562 and GM19238 cell lines, because their entire promoters are not open to TF molecules; other regulatory regions besides the proximal promoters (e.g. intronic enhancers⁴⁶) still enable the TFs to effectively control the expression of the positives with inaccessible promoters. Compared to the other six TFs, the poorer performance of the classifier on YY1 (Table 2) is attributable to its smaller percentage of negatives with inaccessible promoters (Additional file 8²²) and the larger number of functional binding sites in the K562 cell line.

Mutation analyses revealed that some deleterious TFBS mutations could be compensated for by other information-dense clusters in the same promoter (Figure 5, Table 5)^{2,47}; thus, predicting the effects of mutations in individual binding sites might not be sufficient to interpret downstream effects without considering their context. Though other TFBS clusters may compensate and maintain gene expression, the promoter will likely exhibit lower levels of activity than the wild-type promoter, which is a recipe for achieving natural phenotypic diversity⁴⁴. Few published studies in molecular diagnostics have specifically

examined the effects of naturally occurring variants within clustered TFBSs. IDBC-based ML provides an alternative approach to predict deleterious mutations that impact (i.e. repress or abolish) transcription of target genes and result in abnormal phenotypes, and to minimize false positive calls of TFBS variants that alone would be expected to have little or no impact.

Apart from these TFs, the Bray-Curtis Similarity metric can be directly applied to identify the ground-truth genes with overall similar tissue-wide expression patterns to any other gene whose expression profile is known. Previous applications of this index include: a) measurement of the ecological transfer of species abundance from dense to sparse plots⁴⁸, b) comparative difference analyses of species quantities between reference and algorithm-derived metagenomic sample mixtures (<https://precision.fda.gov/challenges/3/view/results>) and c) improvement of friend recommendations in geosocial networks by using it to compare users' movement history^{49,50}.

These results stimulate questions about the biological significance of genes sharing a common expression pattern, including the similarity between other regulatory regions besides proximal promoters in terms of TFBSs and epigenetic markers. This ML framework can also be applied to predict target genes for other TFs and in other cell lines, depending on the availability of corresponding knockdown data.

There are a number of limitations of our approach. The Bray-Curtis function seems unable to accurately measure the similarity between the tissue-wide expression profiles of a gene (e.g. *MIR23A*) without any detectable mRNA in any tissues and genes that are expressed in at least one tissue (e.g. ubiquitously expressed *NR3C1* and stomach-specific *PGA3*). Intuitively, *PGA3* is more similar to *MIR23A* than *NR3C1*; however, the Bray-Curtis similarity indicates that both *PGA3* and *NR3C1* are equally dissimilar to *MIR23A*. The finite number of TFs analyzed is another possible limitation in the prediction of genes with similar expression profiles. This was due to a lack of iPWMs for other TFs that were knocked down. Given that 2000-3000 sequence-specific DNA-binding TFs are estimated to be encoded in the human genome⁵¹, the CRMs of many genes under concerted regulation by different TFs will likely reveal complex circuitry that is currently unknown. For example, the iPWMs for several TFs (CREB, MYB, NF1, GRF1) that bind to the *NR3C1* gene promoter to activate or repress its expression could not be successfully derived from ChIP-seq data^{3,30}. Regarding the CRISPR-generated knockdown data, positives were inferred to be direct targets by intersecting their promoters with corresponding ChIP-seq peaks. This may not be completely accurate, due to the presence of noise peaks that do not contain true TFBSs^{3,52,53}. Small fold changes in the expression levels of DE targets could arise from inefficient knockdown due to suboptimal guide RNAs or to limitations of perturbing only a single allele encoding the TF⁵⁴. Finally, the framework presented considers only the 10 kb interval proximal to the TSS. This could not capture long range enhancer effects beyond this point; a potential way of remediating this would be to incorporate correlation-based approaches that have successfully incorporated multiple definitions of promoter length¹⁵.

Conclusions

We have developed a ML framework with a combination of information theory-based TF binding profiles of the spatial distribution and information contents of TFBS clusters, ChIP-seq and chromatin accessibility data. This framework distinguishes tissue-wide expression profiles of similar vs dissimilar genes (originally defined by the Bray Curtis function) and identified TF targets. Functional binding sites in target genes that significantly alter expression levels upon direct binding are at least partially distinguished by TF-cofactor coregulation from non-functional sites in non-targets. Finally, in-silico mutation analyses suggested that the presence of multiple information-dense clusters in a target gene promoter is capable of mitigating the effects of deleterious mutations that can significantly alter TF-regulated expression levels.

bioRxiv

An earlier version this article is available from bioRxiv: <https://doi.org/10.1101/283267>⁵⁵.

Data availability

Underlying data

The median RPKM, TSS coordinate, DNase I hypersensitivity and ChIP-seq data were respectively obtained from the GTEX Analysis V6p release (www.gtexportal.org), Ensembl Biomart (www.ensembl.org) and ENCODE (www.encodeproject.org). The CRISPR- and siRNA-generated knockdown data were obtained from the supplementary information files of Dixit *et al.*¹⁶ and Cusanovich *et al.*¹⁴. The source datasets generated and/or analysed by this framework, along with sample results and compiled software are available from Zenodo. DOI: <https://doi.org/10.5281/zenodo.1707423>²¹.

Data are available under the terms of the [Creative Commons Zero “No rights reserved” data waiver](https://creativecommons.org/licenses/by/4.0/) (CC0 1.0 Public domain dedication).

Extended data

Additional files are available from Zenodo. DOI: <https://doi.org/10.5281/zenodo.2611953>²².

Additional file 1. The mathematical definitions of the four other similarity metrics, the workflow of the IDBC algorithm, an example feature vector, the mathematical definitions of five statistical variables to measure classifier performance, the default parameter values of classifiers in MATLAB, and histograms visualizing the first two criteria for selecting positives from the CRISPR-generated knockdown data.

Additional file 2: The lists of positives and negatives in the ML classifiers to predict genes with similar tissue-wide expression profiles to *NR3C1*.

Additional file 3: The lists of positives and negatives in the DT classifier to predict TF targets based on the CRISPR-generated knockdown data.

Additional file 4: The lists of positives and negatives in the DT classifier to predict DE direct targets based on the siRNA-generated knockdown data.

Additional file 5: The performance of the DT classifier using only TFBS counts, accuracy of each round of 10-fold cross validation, and Gini importance values of the ML features.

Additional file 6: The list of the most similar 500 PC genes to each TF in terms of tissue-wide expression profiles, and the intersection of these 500 genes and target genes of the TF.

Additional file 7: Cofactor binding sites adjacent to YY1 and EGR1 sites in the promoters of their targets and non-targets.

Additional file 8: The percentages of positives and negatives whose promoters do not overlap DHSs for the CRISPR-perturbed TFs.

Data are available under the terms of the [Creative Commons Zero “No rights reserved” data waiver](https://creativecommons.org/licenses/by/4.0/) (CC0 1.0 Public domain dedication).

Software availability

Source code implementing the ML framework, including generating the figures in this article, is available at: <https://bitbucket.org/cytognomix/information-dense-transcription-factor-binding-site-clusters/>.

Archived source code at time of publication: <https://doi.org/10.5281/zenodo.1892051>⁵⁶.

License: GNU General Public License 3.0.

Grant information

PKR was supported by Natural Sciences and Engineering Research Council of Canada Discovery Grant [RGPIN-2015-06290]; Canada Foundation for Innovation; Canada Research Chairs. RL was supported by a fellowship from the Southern Ontario Smart Computing Innovation Platform, the Ontario Centres of Excellence Talent Edge program and Cytognomix Inc. Compute Canada and Shared Hierarchical Academic Research Computing Network (SHARCNET) provided high performance computing and storage facilities. Funding for open access charge: University of Western Ontario and the Natural Sciences and Engineering Research Council.

The funders had no role in study design, data collection and analysis, decision to publish, or preparation of the manuscript.

Acknowledgements

We are grateful to Ben Shirley and Eliseos Mucaki for constructive comments on the paper.

References

1. Hosseinpour B, Bakhtiarzadeh MR, Khosravi P, *et al.*: **Predicting distinct organization of transcription factor binding sites on the promoter regions: a new genome-based approach to expand human embryonic stem cell regulatory network.** *Gene*. 2013; **531**(2): 212–9.
[PubMed Abstract](#) | [Publisher Full Text](#)
2. Ezer D, Zabet NR, Adryan B: **Homotypic clusters of transcription factor binding sites: A model system for understanding the physical mechanics of gene expression.** *Comput Struct Biotechnol J*. 2014; **10**(17): 63–9.
[PubMed Abstract](#) | [Publisher Full Text](#) | [Free Full Text](#)
3. Lu R, Mucaki EJ, Rogan PK: **Discovery and validation of information theory-based transcription factor and cofactor binding site motifs.** *Nucleic Acids Res*. 2017; **45**(5): e27.
[PubMed Abstract](#) | [Publisher Full Text](#) | [Free Full Text](#)
4. Schneider TD: **Information content of individual genetic sequences.** *J Theor Biol*. 1997; **189**(4): 427–41.
[PubMed Abstract](#) | [Publisher Full Text](#)
5. Dinakarpanth D, Raheja V, Mehta S, *et al.*: **Tandem machine learning for the identification of genes regulated by transcription factors.** *BMC Bioinformatics*. 2005; **6**: 204.
[PubMed Abstract](#) | [Publisher Full Text](#) | [Free Full Text](#)
6. Ouyang Z, Zhou Q, Wong WH: **ChIP-Seq of transcription factors predicts absolute and differential gene expression in embryonic stem cells.** *Proc Natl Acad Sci U S A*. 2009; **106**(51): 21521–6.
[PubMed Abstract](#) | [Publisher Full Text](#) | [Free Full Text](#)
7. Cheng C, Alexander R, Min R, *et al.*: **Understanding transcriptional regulation by integrative analysis of transcription factor binding data.** *Genome Res*. 2012; **22**(9): 1658–67.
[PubMed Abstract](#) | [Publisher Full Text](#) | [Free Full Text](#)
8. Budden DM, Hurley DG, Cursons J, *et al.*: **Predicting expression: the complementary power of histone modification and transcription factor binding data.** *Epigenetics Chromatin*. 2014; **7**(1): 36.
[PubMed Abstract](#) | [Publisher Full Text](#) | [Free Full Text](#)
9. Smith AD, Sumazin P, Xuan Z, *et al.*: **DNA motifs in human and mouse proximal promoters predict tissue-specific expression.** *Proc Natl Acad Sci U S A*. 2006; **103**(16): 6275–80.
[PubMed Abstract](#) | [Publisher Full Text](#) | [Free Full Text](#)
10. Zabet NR, Adryan B: **Estimating binding properties of transcription factors from genome-wide binding profiles.** *Nucleic Acids Res*. 2015; **43**(1): 84–94.
[PubMed Abstract](#) | [Publisher Full Text](#) | [Free Full Text](#)
11. McLeay RC, Lesluyes T, Cuellar Partida G, *et al.*: **Genome-wide *in silico* prediction of gene expression.** *Bioinformatics*. 2012; **28**(21): 2789–96.
[PubMed Abstract](#) | [Publisher Full Text](#) | [Free Full Text](#)
12. Karlič R, Chung HR, Lasserre J, *et al.*: **Histone modification levels are predictive for gene expression.** *Proc Natl Acad Sci U S A*. 2010; **107**(7): 2926–31.
[PubMed Abstract](#) | [Publisher Full Text](#) | [Free Full Text](#)
13. Dong X, Greven MC, Kundaje A, *et al.*: **Modeling gene expression using chromatin features in various cellular contexts.** *Genome Biol*. 2012; **13**(9): R53.
[PubMed Abstract](#) | [Publisher Full Text](#) | [Free Full Text](#)
14. Cusanovich DA, Pavlovic B, Pritchard JK, *et al.*: **The functional consequences of variation in transcription factor binding.** *PLoS Genet*. 2014; **10**(3): e1004226.
[PubMed Abstract](#) | [Publisher Full Text](#) | [Free Full Text](#)
15. Banks CJ, Joshi A, Michael T: **Functional transcription factor target discovery via compendia of binding and expression profiles.** *Sci Rep*. 2016; **6**: 20649.
[PubMed Abstract](#) | [Publisher Full Text](#) | [Free Full Text](#)
16. Dixit A, Parnas O, Li B, *et al.*: **Perturb-Seq: Dissecting Molecular Circuits with Scalable Single-Cell RNA Profiling of Pooled Genetic Screens.** *Cell*. 2016; **167**(7): 1853–1866.e17.
[PubMed Abstract](#) | [Publisher Full Text](#) | [Free Full Text](#)
17. Cui S, Youn E, Lee J, *et al.*: **An improved systematic approach to predicting transcription factor target genes using support vector machine.** *PLoS One*. 2014; **9**(4): e94519.
[PubMed Abstract](#) | [Publisher Full Text](#) | [Free Full Text](#)
18. Bray JR, Curtis JT: **An Ordination of the Upland Forest Communities of Southern Wisconsin.** *Ecol Monogr*. 1957; **27**(4): 325–349.
[Publisher Full Text](#)
19. International Human Genome Sequencing Consortium: **Finishing the euchromatic sequence of the human genome.** *Nature*. 2004; **431**(7011): 931–45.
[PubMed Abstract](#) | [Publisher Full Text](#)
20. GTEx Consortium: **The Genotype-Tissue Expression (GTEx) project.** *Nat Genet*. 2013; **45**(6): 580–5.
[PubMed Abstract](#) | [Publisher Full Text](#) | [Free Full Text](#)
21. Lu R, Rogan PK: **Information-dense transcription factor binding site clusters identify target genes with similar tissue-wide expression profiles and serve as a buffer against mutations - Source datasets, sample results and compiled software.** 2018.
<http://www.doi.org/10.5281/zenodo.1707423>
22. Lu R, Rogan PK: **Information-dense transcription factor binding site clusters identify target genes with similar tissue-wide expression profiles and serve as a buffer against mutations - Additional files.** 2018.
<http://www.doi.org/10.5281/zenodo.2611953>
23. ENCODE Project Consortium: **An integrated encyclopedia of DNA elements in the human genome.** *Nature*. 2012; **489**(7414): 57–74.
[PubMed Abstract](#) | [Publisher Full Text](#) | [Free Full Text](#)
24. Thurman RE, Rynes E, Humbert R, *et al.*: **The accessible chromatin landscape of the human genome.** *Nature*. 2012; **489**(7414): 75–82.
[PubMed Abstract](#) | [Publisher Full Text](#) | [Free Full Text](#)
25. Pearson K: **Note on Regression and Inheritance in the Case of Two Parents.** *Proc R Soc Lond*. 1895; **58**: 240–2.
[Publisher Full Text](#)
26. Spearman C: **The Proof and Measurement of Association between Two Things.** *Am J Psychol*. 1904; **15**(1): 72–101.
[Publisher Full Text](#)
27. He H, Garcia EA: **Learning from Imbalanced Data.** *IEEE Trans Knowl Data Eng*. 2009; **21**(9): 1263–1284.
[Publisher Full Text](#)
28. Kent WJ, Sugnet CW, Furey TS, *et al.*: **The human genome browser at UCSC.** *Genome Res*. 2002; **12**(6): 996–1006.
[PubMed Abstract](#) | [Publisher Full Text](#) | [Free Full Text](#)
29. Sherry ST, Ward MH, Kholodov M, *et al.*: **dbSNP: the NCBI database of genetic variation.** *Nucleic Acids Res*. 2001; **29**(1): 308–11.
[PubMed Abstract](#) | [Publisher Full Text](#) | [Free Full Text](#)
30. Vandevyver S, Dejager L, Libert C: **Comprehensive overview of the structure and regulation of the glucocorticoid receptor.** *Endocr Rev*. 2014; **35**(4): 671–93.
[PubMed Abstract](#) | [Publisher Full Text](#)
31. Kaplan T, Li XY, Sabo PJ, *et al.*: **Quantitative models of the mechanisms that control genome-wide patterns of transcription factor binding during early *Drosophila* development.** *PLoS Genet*. 2011; **7**(2): e1001290.
[PubMed Abstract](#) | [Publisher Full Text](#) | [Free Full Text](#)
32. Simicevic J, Schmid AW, Gilardoni PA, *et al.*: **Absolute quantification of transcription factors during cellular differentiation using multiplexed targeted proteomics.** *Nat Methods*. 2013; **10**(6): 570–6.
[PubMed Abstract](#) | [Publisher Full Text](#)
33. Calvo SE, Clauser KR, Mootha VK: **MitoCarta2.0: an updated inventory of mammalian mitochondrial proteins.** *Nucleic Acids Res*. 2016; **44**(D1): D1251–1257.
[PubMed Abstract](#) | [Publisher Full Text](#) | [Free Full Text](#)
34. Cunningham JT, Rodgers JT, Arlow DH, *et al.*: **mTOR controls mitochondrial oxidative function through a YY1-PGC-1 α transcriptional complex.** *Nature*. 2007; **450**(7170): 736–40.
[PubMed Abstract](#) | [Publisher Full Text](#)
35. Tallack MR, Perkins AC: **KLF1 directly coordinates almost all aspects of terminal erythroid differentiation.** *IUBMB Life*. 2010; **62**(12): 886–90.
[PubMed Abstract](#) | [Publisher Full Text](#)
36. Seto E, Lewis B, Shenk T: **Interaction between transcription factors Sp1 and YY1.** *Nature*. 1993; **365**(6445): 462–4.
[PubMed Abstract](#) | [Publisher Full Text](#)
37. Ferrari-Amorotti G, Mariani SA, Novi C, *et al.*: **The biological effects of C/EBP α in K562 cells depend on the potency of the N-terminal regulatory region, not on specificity of the DNA binding domain.** *J Biol Chem*. 2010; **285**(40): 30837–50.
[PubMed Abstract](#) | [Publisher Full Text](#) | [Free Full Text](#)
38. Huang RP, Fan Y, Ni Z, *et al.*: **Reciprocal modulation between Sp1 and Egr-1.** *J Cell Biochem*. 1997; **66**(4): 489–99.
[PubMed Abstract](#) | [Publisher Full Text](#)
39. Bell AC, West AG, Felsenfeld G: **The protein CTCF is required for the enhancer blocking activity of vertebrate insulators.** *Cell*. 1999; **98**(3): 387–96.
[PubMed Abstract](#) | [Publisher Full Text](#)
40. Hou C, Zhao H, Tanimoto K, *et al.*: **CTCF-dependent enhancer-blocking by alternative chromatin loop formation.** *Proc Natl Acad Sci U S A*. 2008; **105**(51): 20398–403.
[PubMed Abstract](#) | [Publisher Full Text](#) | [Free Full Text](#)
41. Wang LC, Swat W, Fujiwara Y, *et al.*: **The TEL/ETV6 gene is required specifically for hematopoiesis in the bone marrow.** *Genes Dev*. 1998; **12**(15): 2392–402.
[PubMed Abstract](#) | [Publisher Full Text](#) | [Free Full Text](#)
42. Tian L, Liu J, Xia GH, *et al.*: **RNAi-mediated knockdown of MCM7 gene on CML cells and its therapeutic potential for leukemia.** *Med Oncol*. 2017; **34**(2): 21.
[PubMed Abstract](#) | [Publisher Full Text](#)
43. Maifrede S, Liebermann D, Hoffman B: **Egr-1, a Stress Response Transcription Factor and Myeloid Differentiation Primary Response Gene, Behaves As Tumor Suppressor in CML.** *Blood*. 2014; **124**: 2211.
[Reference Source](#)
44. Smith T, Husband P, Layzell P, *et al.*: **Fitness landscapes and evolvability.** *Evol Comput*. 2002; **10**(1): 1–34.
[PubMed Abstract](#) | [Publisher Full Text](#)

45. Kimura M: **The neutral theory of molecular evolution.** *Sci Am.* 1979; **241**(5): 98–100, 102, 108 passim.
[PubMed Abstract](#)
46. Hural JA, Kwan M, Henkel G, *et al.*: **An intron transcriptional enhancer element regulates IL-4 gene locus accessibility in mast cells.** *J Immunol.* 2000; **165**(6): 3239–49.
[PubMed Abstract](#) | [Publisher Full Text](#)
47. Ma X, Ezer D, Adryan B, *et al.*: **Canonical and single-cell Hi-C reveal distinct chromatin interaction sub-networks of mammalian transcription factors.** *Genome Biol.* 2018; **19**(1): 174.
[PubMed Abstract](#) | [Publisher Full Text](#) | [Free Full Text](#)
48. Ricotta C, Podani J: **On some properties of the Bray-Curtis dissimilarity and their ecological meaning.** *Ecological Complexity.* 2017; **31**: 201–205.
[Publisher Full Text](#)
49. Chen X, Lu R, Ma X, *et al.*: **Measuring User Similarity with Trajectory Patterns: Principles and New Metrics.** *APWeb.* 2014; **8709**: 437–448.
[Publisher Full Text](#)
50. Chen X, Krody P, Lu R, *et al.*: **MinUS: Mining User Similarity with Trajectory Patterns.** *ECML PKDD.* 2014; **8726**: 436–439.
[Publisher Full Text](#)
51. Vaquerizas JM, Kummerfeld SK, Teichmann SA, *et al.*: **A census of human transcription factors: function, expression and evolution.** *Nat Rev Genet.* 2009; **10**(4): 252–63.
[PubMed Abstract](#) | [Publisher Full Text](#)
52. Kidder BL, Hu G, Zhao K: **CHIP-Seq: technical considerations for obtaining high-quality data.** *Nat Immunol.* 2011; **12**(10): 918–22.
[PubMed Abstract](#) | [Publisher Full Text](#) | [Free Full Text](#)
53. Teytelman L, Thurtle DM, Rine J, *et al.*: **Highly expressed loci are vulnerable to misleading CHIP localization of multiple unrelated proteins.** *Proc Natl Acad Sci U S A.* 2013; **110**(46): 18602–7.
[PubMed Abstract](#) | [Publisher Full Text](#) | [Free Full Text](#)
54. Shao Y, Chan CY, Maliyekkel A, *et al.*: **Effect of target secondary structure on RNAi efficiency.** *RNA.* 2007; **13**(10): 1631–40.
[PubMed Abstract](#) | [Publisher Full Text](#) | [Free Full Text](#)
55. Lu R, Rogan PK: **Information-dense transcription factor binding site clusters identify target genes with similar tissue-wide expression profiles and serve as a buffer against mutations.** *bioRxiv.* 2018; 283267.
[Publisher Full Text](#)
56. Lu R, Rogan PK: **Information dense transcription factor binding site clusters identify target genes with similar tissue-wide expression profiles and buffer against mutations - source code.** *Zenodo.* 2018.
<http://www.doi.org/10.5281/zenodo.1892051>

Open Peer Review

Current Referee Status:  

Version 2

Referee Report 11 April 2019

<https://doi.org/10.5256/f1000research.20525.r46854>



Daphne Ezer 

The Alan Turing Institute for Data Science, London, UK

Most of the comments were addressed. I still have reservations about point #2 from my previous report - the authors just repeated that their approach fits the definition of a distance metric (which is true), but I think that many biologists would find it counter-intuitive that two genes with very different gene expression *patterns* over different tissues, but with the same mean expression value would be considered 'closer' than two genes that have the same "pattern" of gene expression across tissues but very different raw gene expression values.

However, I now suggest that the authors consider writing a follow-up paper about this, rather than address this point within this manuscript.

Competing Interests: No competing interests were disclosed.

Reviewer Expertise: bioinformatics; transcriptional regulation

I have read this submission. I believe that I have an appropriate level of expertise to confirm that it is of an acceptable scientific standard.

Referee Report 09 April 2019

<https://doi.org/10.5256/f1000research.20525.r46855>



Nicolae Radu Zabet 

School of Biological Sciences, University of Essex, Colchester, UK

The authors have addressed all my comments.

Competing Interests: No competing interests were disclosed.

Reviewer Expertise: genomics, chromatin biology, transcription regulation, bioinformatics, statistical models,

I have read this submission. I believe that I have an appropriate level of expertise to confirm that it is of an acceptable scientific standard.

Version 1

Referee Report 08 February 2019

<https://doi.org/10.5256/f1000research.18988.r42457>**Nicolae Radu Zabet**

School of Biological Sciences, University of Essex, Colchester, UK

In this manuscript, Ru and Rogan use Bray-Curtis Similarity and several machine-learning algorithms to identify genes that have similar expression patterns. They use transcription factor binding sites within promoter regions and DNA accessibility data to train their models. This is a very important question and the authors propose an interesting mechanistic approach to address it. Nevertheless, there are several limitations that need to be addressed.

Specific comments:

1. While the grammar is at a good level, the way the information is presented makes the text very difficult to read. Some sentences are very long and there are many notations. One suggestion is to move some of the less important parts in the Supplementary Material.
2. On page 3 in the introduction, the authors claim that signal strength of ChIP-seq peaks are not strictly proportional to TF binding strength. This is not always true and we showed in¹ that in fact the number of TF molecules controls the height of the ChIP-seq peak.
3. On page 5, it is not clear why the authors talk of Features 1-3, since it seemed they had 7 features. The way the machine learning information is presented should be improved.
4. The authors test Naïve Bayes, Decision Tree, Random Forest and SVM. I was wondering if they consider also Neural Networks. They don't need to implement that now, but they should at least mention what was behind their selection for the machine-learning algorithms.
5. One of the main findings is that DNA accessibility improves predictions, because it masks potential TF binding sites. This is something that was previously showed in the context of TF binding to the genome by us and other scientists (e.g. References 1,2,3).
6. Figure 4 needs re-plotting (e.g. x axis labels do not fit the figure).
7. In the discussion, none of the statements are referred back to any of the figures in the results section. This makes the reading difficult.
8. The lower performance for YY1 needs to be better explained. The authors claim that this could be explained by lower percentage of negatives in inaccessible promoters. Are there other examples of TFs displaying similar features? What is their performance?
9. One of the main limitations of the manuscript is that the authors use only 82 TFs and claim that there are no iPWM for others. Have they tried to use MotifDB (<https://bioconductor.org/packages/release/bioc/html/MotifDb.html>), which has approximately 1000 PWMs for human TFs?
10. When talking about the accuracy of the ChIP-seq signal, they could also reference this paper⁴.

References

1. Zabet NR, Adryan B: Estimating binding properties of transcription factors from genome-wide binding profiles. *Nucleic Acids Res.* 2015; **43** (1): 84-94 [PubMed Abstract](#) | [Publisher Full Text](#)

2. Kaplan T, Li XY, Sabo PJ, Thomas S, Stamatoyannopoulos JA, Biggin MD, Eisen MB: Quantitative models of the mechanisms that control genome-wide patterns of transcription factor binding during early *Drosophila* development. *PLoS Genet.* 2011; **7** (2): e1001290 [PubMed Abstract](#) | [Publisher Full Text](#)
3. Simicevic J, Schmid AW, Gilardoni PA, Zoller B, Raghav SK, Krier I, Gubelmann C, Lisacek F, Naef F, Moniatte M, Deplancke B: Absolute quantification of transcription factors during cellular differentiation using multiplexed targeted proteomics. *Nat Methods.* 2013; **10** (6): 570-6 [PubMed Abstract](#) | [Publisher Full Text](#)
4. Teytelman L, Thurtle DM, Rine J, van Oudenaarden A: Highly expressed loci are vulnerable to misleading ChIP localization of multiple unrelated proteins. *Proc Natl Acad Sci U S A.* 2013; **110** (46): 18602-7 [PubMed Abstract](#) | [Publisher Full Text](#)

Is the work clearly and accurately presented and does it cite the current literature?

Partly

Is the work clearly and accurately presented and does it cite the current literature?

Partly

Is the study design appropriate and is the work technically sound?

Yes

Is the study design appropriate and is the work technically sound?

Yes

Are sufficient details of methods and analysis provided to allow replication by others?

Partly

Are sufficient details of methods and analysis provided to allow replication by others?

Partly

If applicable, is the statistical analysis and its interpretation appropriate?

Yes

If applicable, is the statistical analysis and its interpretation appropriate?

Yes

Are all the source data underlying the results available to ensure full reproducibility?

Yes

Are all the source data underlying the results available to ensure full reproducibility?

Yes

Are the conclusions drawn adequately supported by the results?

Partly

Are the conclusions drawn adequately supported by the results?

Partly

Competing Interests: No competing interests were disclosed.

Reviewer Expertise: genomics, chromatin biology, transcription regulation, bioinformatics, statistical models,

I have read this submission. I believe that I have an appropriate level of expertise to confirm that it is of an acceptable scientific standard, however I have significant reservations, as outlined above.

Author Response 25 Mar 2019

Peter Rogan, University of Western Ontario, Canada

Comment 1: While the grammar is at a good level, the way the information is presented makes the text very difficult to read. Some sentences are very long and there are many notations. One suggestion is to move some of the less important parts in the Supplementary Material.

Response: The manuscript has been extensively edited to improve clarity of the presentation. Sentence lengths have been reduced. Duplicate terms and text have been eliminated. All abbreviations have been defined. Two paragraphs have been moved to the Supplementary Methods. The revised manuscript has been shortened by 400 words and approximately 2 pages.

Comment 2: On page 3 in the introduction, the authors claim that signal strength of ChIP-seq peaks are not strictly proportional to TF binding strength. This is not always true and we showed in ¹ that in fact the number of TF molecules controls the height of the ChIP-seq peak.

Response: In (1), it was discovered that signal strengths of ChIP-seq peaks are not strictly proportional to strengths (R_i values) of the strongest TFBSs contained in the peaks. The finding in (2) provides a complementary explanation about the determinants of signal strengths of ChIP-seq peaks, which is that 'the number of TF molecules controls the height of the ChIP-seq peak'. Therefore, this sentence is revised to "Because signal strengths of ChIP-seq peaks are not strictly proportional to strengths of the contained strongest TFBSs and are instead controlled by TFBS counts [3, 10], representing...".

Comment 3: On page 5, it is not clear why the authors talk of Features 1-3, since it seemed they had 7 features. The way the machine learning information is presented should be improved.

Response: In this sentence, we would like to make it easier for readers to understand the generation of classifier predictors, by explaining how the seven high-level features were transformed to low-level predictors that were directly input into the classifiers. Therefore, this sentence was revised to "Each of the Features 1-3 was defined in a gene as a vector, whose size equals the number of clusters in the gene promoter; each cluster was mapped to a single value in the vector. In Features 4-7, each cluster itself was mapped to a vector corresponding to binding sites for 82 TFs (Additional file 1)." Also, Section 5 of Additional file 1 gives a specific example about the predictor vector of a gene instance.

Comment 4: The authors test Naïve Bayes, Decision Tree, Random Forest and SVM. I was wondering if they consider also Neural Networks. They don't need to implement that now, but they should at least mention what was behind their selection for the machine-learning algorithms.

Response: We did not select Neural Networks due to two considerations. First, it requires much more data to train than traditional machine learning algorithms, as in at least thousands if not millions of labeled samples (3). In this study the numbers of both positives (i.e. protein-coding genes with similar tissue-wide expression profiles to *NR3C1*) and negatives (i.e. dissimilar genes) are 500, which is insufficient to apply Neural Networks. Second, it is more computationally

expensive than traditional algorithms (4).

Comment 5: One of the main findings is that DNA accessibility improves predictions, because it masks potential TF binding sites. This is something that was previously showed in the context of TF binding to the genome by us and other scientists (e.g. References 1,2,3).

Response: Accordingly, in this revision, the last sentence of the second subsection of the Results section was revised to “Consistent with previous findings (2, 5, 6), inclusion of DHS information significantly improved AUC values of the other classifiers with the exception of Naïve Bayes.”. And in the second paragraph of the Discussion section, the second sentence was revised to “This intersection eliminated noisy binding sites that are inaccessible to TF proteins in promoters (2, 5, 6),...”

Comment 6: Figure 4 needs re-plotting (e.g. x axis labels do not fit the figure).

Response: In this revision, Figure 4 was replotted to fix this issue.

Comment 7: In the discussion, none of the statements are referred back to any of the figures in the results section. This makes the reading difficult.

Response: In the first paragraph of the Discussion section of this revision, references to the figures in the Results section were added to the following sentences, “In this study, the Bray-Curtis similarity function was initially shown (for the NR3C1 gene) to measure the relatedness of overall expression patterns between genes across a diverse set of tissues (Figure 2). A ML framework distinguished similar from dissimilar genes based on the distribution, strengths and compositions of TFBS clusters in accessible promoters, which can substantially account for the corresponding gene expression patterns (Figures 1 & 3). Using gene expression knockdown data, the combinatorial use of TF binding profiles and chromatin accessibility was also demonstrated to be predictive of TF targets (Figure 4, Tables 2 & 3). A binding site comparison confirmed that coregulatory cofactors can be used to distinguish between functional sites in targets and non-functional ones in non-targets. Furthermore, in silico mutation analyses on binding sites of targets suggested that the existence of both multiple TFBSs in a cluster and multiple information-dense clusters in the same promoter enables both the cluster and the promoter to be resilient to mutations in individual TFBS (Figure 5, Table 5).”

In the third paragraph, references to the figures in the Results section were added to the following sentence, “Mutation analyses revealed that some deleterious TFBS mutations could be compensated for by other information-dense clusters in the same promoter (Figure 5, Table 5)”

Comment 8: The lower performance for YY1 needs to be better explained. The authors claim that this could be explained by lower percentage of negatives in inaccessible promoters. Are there other examples of TFs displaying similar features? What is their performance?

Response: In this sentence, all the seven CRISPR-perturbed TFs were split into two sets; one consisting of only YY1, the other consisting of the remaining six TFs. This sentence was comparing the performances of the Decision Tree classifiers on these two TF sets. Seen from Table 3, the classifier’s performance on YY1 was markedly lower than that on the other six TFs after intersecting promoters with DHS sites, which is due to the fact that YY1 has a smaller percentage of negatives with inaccessible promoters.

To make this clearer, in this revision, this sentence was revised to “Compared to the other six TFs, the poorer performance of the classifier on YY1 (Table 2) is attributable to ...”

Comment 9: One of the main limitations of the manuscript is that the authors use only 82 TFs and

claim that there are no iPWM for others. Have they tried to use MotifDB (<https://bioconductor.org/packages/release/bioc/html/MotifDb.html>), which has approximately 1000 PWMs for human TFs?

Response: We selected to use these 94 iPWMs of 82 TFs that were derived from ENCODE ChIP-seq datasets using entropy minimization in (1), since we want to ensure the high quality of the iPWMs used in the analyses.

Compared to the MotifDB PWMs, the reliability and accuracy of these iPWMs were extensively and independently validated using four methods, including detection of experimentally proven binding sites, explanation of effects of characterized SNPs, comparison with previously published motifs and statistical analyses.

These iPWMs were used to scan for 803 experimentally confirmed TFBSs, and there was complete concordance between these true binding sites and those detected with the iPWMs, both in terms of their locations and relative strengths (1). And these iPWMs were further used to explain the experimentally observed effects of 153 SNPs on binding site strengths, based on the changes in the R_j values. For 130 SNPs (~85.0%), the predictions of the iPWMs and the experimental observations are completely concordant; for 16 SNPs (~10.5%), the predicted and observed experimental findings are concordant, but the extents of these changes differ (e.g. TF binding is predicted to only be weakened, but binding was completely abolished in experiments); for only 7 SNPs (~4.6%), the predicted and observed experimental changes were discordant.

The PWMs in MotifDB are not information theory-based (i.e. not iPWMs). Instead, they are given in the form of count matrices or frequency matrices. The performance of the iPWMs that used in the present study has been shown to outperform other PWM-based approaches for binding site detection and quantification (7).

Comment 10: When talking about the accuracy of the ChIP-seq signal, they could also reference this paper⁴.

Response: In this revision, the reference was added to the following sentence in the last paragraph of the Discussion section, “Regarding the CRISPR-generated knockdown data, positives were inferred to be direct targets by intersecting their promoters with corresponding ChIP-seq peaks. This may not be completely accurate, due to the presence of noise peaks that do not contain true TFBSs^{3, 50, 51}.”

References:

1. Lu, R., Mucaki, E.J. and Rogan, P.K. (2017) Discovery and validation of information theory-based transcription factor and cofactor binding site motifs. *Nucleic Acids Res.*, **45**, e27.
2. Zabet, N.R. and Adryan, B. (2015) Estimating binding properties of transcription factors from genome-wide binding profiles. *Nucleic Acids Res.*, **43**, 84–94.
3. Zhang, Y. and Yang, Q. (2017) A Survey on Multi-Task Learning. *ArXiv170708114 Cs*.
4. Ghodsi, Z., Gu, T. and Garg, S. (2017) SafetyNets: Verifiable execution of deep neural networks on an untrusted cloud. In *Advances in Neural Information Processing Systems*. Vol. 2017-December, pp. 4673–4682.
5. Kaplan, T., Li, X.-Y., Sabo, P.J., Thomas, S., Stamatoyannopoulos, J.A., Biggin, M.D. and Eisen, M.B. (2011) Quantitative models of the mechanisms that control genome-wide patterns of transcription factor binding during early *Drosophila* development. *PLoS Genet.*, **7**, e1001290.
6. Simicevic, J., Schmid, A.W., Gilardoni, P.A., Zoller, B., Raghav, S.K., Krier, I., Gubelmann, C.,

Lisacek, F., Naef, F., Moniatte, M., *et al.* (2013) Absolute quantification of transcription factors during cellular differentiation using multiplexed targeted proteomics. *Nat. Methods*, **10**, 570–576.
7. Erill I and O'Neill MC. (2009) A reexamination of information theory-based methods for DNA binding site identification. *BMC Bioinformatics*, **10**, 57.

Competing Interests: None

Referee Report 09 January 2019

<https://doi.org/10.5256/f1000research.18988.r42458>



Daphne Ezer 

The Alan Turing Institute for Data Science, London, UK

I think that this is an interesting paper that should be published. Often, gene expression patterns are clustered and TF binding sites are used as features to build a classifier for identifying the cluster to which those genes belong or similar schemes such as clustering TFs and gene expression together- see Clements *et al*¹ and Berman *et al*². However, a biologist may want to identify what TFs regulate a specific gene of interest. They could then use the 'Bray-Curtis Similarity' index to find a set of genes whose expression pattern is similar to their gene of interest. Then, they can use the pipeline presented here to identify features that are predictive of this kind of gene expression pattern.

They also create a scheme to test how different combinations of features from different experiments influence their predictions.

I think that the text would garner much more interest if it focused more on the research questions that are being addressed. The method details are discussed in depth, but the big picture is hard to find amidst the details.

Main points:

1. One of the main things that bothers me about the Bray-Curtis Similarity metric is that it seems to assume that tissues are independently sampled. However, we see from Fig.1 that there are many brain samples that seem to (at least in the three genes shown) have similar gene expression values. Is there a lot of covariance between gene expression values in pairs of tissues? If so, is there a way to adjust this metric to acknowledge stratification of the tissues. I don't think that the whole paper needs to be re-written with a new metric, but it would be nice if the authors address this directly.
2. Another issue I have is with this metric is that it uses RPKM gene expression values in the Bray-Curtis Similarity metric. Imagine that two genes have extremely high gene expression values in some tissue (like the brain) and low values in another tissue (like the pancreas). However, one of these genes is always expressed at 10 times the level of the other gene. Lets say that a third gene has almost no change of gene expression value across the tissues but has a mean RPKM that is

similar to the first gene's mean RPKM. Would the Bray-Curtis Similarity metric say that gene 1 and 2 are more similar? Or gene 1 and 3? If gene 1 and 3, then this might be resolved by comparing z-scores or otherwise normalising gene expression values across tissues.

3. Every time a machine learning method is named, it should be clear: (1) what are the input features (ii) what are the labels -- i.e. what is being classified (iii) what is the cross-validation or training-testing-validation scheme. Since there are so many machine learning things being done, it is hard sometimes to make sense of what is being done in each specific case.
4. For the method described in (B) in Fig 1: Does it necessarily make sense to compare the 'most similar' to the 'least similar'? Genes that have exactly the opposite gene expression pattern to the one you are interested might be tightly regulated by a different set of TFs. You might be picking up this signal instead of the one you care about! This might be an even bigger issue since you are using raw gene expression values-- genes that are very highly or very lowly expressed in all tissues might always come up in your negative set.
5. Biologists don't just want good classifiers, they want feature selection! Can you show the Gini scores of the features in a supplemental table?

Smaller changes:

1. Is all the code for generating every figure available online? Let's help make research reproducible.
2. If you have 10 values (from cross validation), why don't you show them all in Figure 4 so we can evaluate the spread.
3. "Our *in-silico* mutation analyses revealed that some deleterious TFBS mutations could be compensated for by other information-dense clusters in the same promoter²; thus, predicting the effects of mutations in individual binding sites might not be sufficient to interpret downstream effects without considering their context." This is something that me and my collaborators have recently studied³. Don't feel pressure to add this citation-- I just thought it would be interesting for you to read! (Also, thanks for discussing IDBC in this paper-- I hadn't heard of it before but it would be relevant to my research.)
4. It would be great if you discussed how Bray-Curtis is used in other fields in the Discussion.
5. Better subsection names in the results section - emphasizing the biological conclusions rather than what was done.

References

1. Clements M, van Someren EP, Knijnenburg TA, Reinders MJ: Integration of known transcription factor binding site information and gene expression data to advance from co-expression to co-regulation. *Genomics Proteomics Bioinformatics*. 2007; **5** (2): 86-101 [PubMed Abstract](#) | [Publisher Full Text](#)
2. Berman BP, Nibu Y, Pfeiffer BD, Tomancak P, Celniker SE, Levine M, Rubin GM, Eisen MB: Exploiting transcription factor binding site clustering to identify cis-regulatory modules involved in pattern formation in the *Drosophila* genome. *Proc Natl Acad Sci U S A*. 2002; **99** (2): 757-62 [PubMed Abstract](#) | [Publisher Full Text](#)
3. Ma X, Ezer D, Adryan B, Stevens T: Canonical and single-cell Hi-C reveal distinct chromatin interaction sub-networks of mammalian transcription factors. *Genome Biology*. 2018; **19** (1). [Publisher Full Text](#)

Is the work clearly and accurately presented and does it cite the current literature?

Partly

Is the work clearly and accurately presented and does it cite the current literature?

Partly

Is the study design appropriate and is the work technically sound?

Yes

Is the study design appropriate and is the work technically sound?

Yes

Are sufficient details of methods and analysis provided to allow replication by others?

Yes

Are sufficient details of methods and analysis provided to allow replication by others?

Yes

If applicable, is the statistical analysis and its interpretation appropriate?

Partly

If applicable, is the statistical analysis and its interpretation appropriate?

Partly

Are all the source data underlying the results available to ensure full reproducibility?

Yes

Are all the source data underlying the results available to ensure full reproducibility?

Yes

Are the conclusions drawn adequately supported by the results?

Partly

Are the conclusions drawn adequately supported by the results?

Partly

Competing Interests: No competing interests were disclosed.

Reviewer Expertise: bioinformatics; transcriptional regulation

I have read this submission. I believe that I have an appropriate level of expertise to confirm that it is of an acceptable scientific standard, however I have significant reservations, as outlined above.

Author Response 25 Mar 2019

Peter Rogan, University of Western Ontario, Canada

Comment 1: One of the main things that bothers me about the Bray-Curtis Similarity metric is that it seems to assume that tissues are independently sampled. However, we see from Fig.1 that there are many brain samples that seem to (at least in the three genes shown) have similar gene expression values. Is there a lot of covariance between gene expression values in pairs of tissues? If so, is there a way to adjust this metric to acknowledge stratification of the tissues. I don't think that the whole paper needs to be re-written with a new metric, but it would be nice if the authors address this directly.

Response: There are 13 brain tissues among all the 53 tissues investigated by GTE_x. Admittedly,

genes tend to exhibit closer expression values between some of these brain tissues; for example, seen from Figure 2, the *NR3C1* gene has close, low expression values in multiple brain tissues (Amygdala, Anterior cingulate cortex (BA24), Caudate (basal ganglia), etc).

To investigate how much this covariance can influence similarity values between tissue-wide expression profiles of genes computed by the Bray-Curtis function, using the brain tissues as an example, we retained only one brain tissue and removed all other brain tissues at one time, and recomputed the Bray-Curtis similarity values between *NR3C1* and all other protein-coding genes. Thus, there are 13 variant cases due to the presence of 13 brain tissues. Then we compared the resultant set of 500 most similar genes in each variant case to that when all 53 tissues were used (given in Additional file 2).

All of the top 100 most similar genes when using all 53 tissues were among the top 500 genes in every variant case. The top 200 genes when using all 53 tissues differed by 0-3 genes from the top 500 genes in variant cases. The top 500 genes when using all 53 tissues differed by approximately 22% (112-117) from top 500 genes in variant cases. This suggests that the increased number of brain tissues does not significantly influence the results of the Bray-Curtis metric for the most similar genes but does affect results at lower similarity threshold.

Especially, in all 14 cases (i.e. the 13 variant cases and using all 53 tissues), the three most similar genes to *NR3C1* are the same (*SLC25A32*, *TANK*, *CDC27*). Therefore, this covariance between these brain tissues is not a dominant factor in identifying genes with similar tissue-wide expression profiles to a particular gene using the Bray-Curtis Function.

On the other hand, the situation is also present that a gene has closer expression values between two tissues from two different organs, than between two more similar tissues from the same organ. For example, both the Cerebellar Hemisphere (CH) tissue and the Amygdala tissue are from the brain; the Visceral Adipose (VA) tissue and the Adrenal Gland (AG) tissue are not. Seen from Figure 2, for the *NR3C1* gene's expression, there is a larger difference between CH and Amygdala. Instead, CH is closer to VA, whereas Amygdala is closer to AG.

Despite well established developmental lineages for these tissues, we prefer not to make assumptions regarding the covariance in expression values between similar tissues from the same organ. The null hypothesis should not discriminate between tissues or weight them differently, without explicit prior information about tissue-specific expression, which is what we are trying to measure. For this reason, when computing similarity values between tissue-wide expression profiles of genes using the Bray-Curtis Function or other metrics, it may be more appropriate to assign the same weight to every tissue and treat every tissue equally.

Comment 2: Another issue I have is with this metric is that it uses RPKM gene expression values in the Bray-Curtis Similarity metric. Imagine that two genes have extremely high gene expression values in some tissue (like the brain) and low values in another tissue (like the pancreas). However, one of these genes is always expressed at 10 times the level of the other gene. Lets say that a third gene has almost no change of gene expression value across the tissues but has a mean RPKM that is similar to the first gene's mean RPKM. Would the Bray-Curtis Similarity metric say that gene 1 and 2 are more similar? Or gene 1 and 3? If gene 1 and 3, then this might be resolved by comparing z-scores or otherwise normalising gene expression values across tissues.

Response:

Gene 1 and 3 will be more similar according to Bray-Curtis Similarity. The inference is as follows: Assume that there are two tissues t_1 and t_2 . The expression values of Gene 1 in the two tissues are $[a, b]$ ($b \gg a > 0$), the expression values of Gene 2 are $[10a, 10b]$, and the expression values of Gene 3 are $[(a+b)/2, (a+b)/2]$.

Then the Bray-Curtis similarity value between Gene 1 and Gene 2 is:

$$\text{sim}_{BC}(G1, G2) = 2/11.$$

The Bray-Curtis similarity value between Gene 1 and Gene 3 is:

$$\text{sim}_{BC}(G1, G3) = (3a+b)/(2a+2b).$$

Thus, $\text{sim}_{BC}(G1, G3) > \text{sim}_{BC}(G1, G2)$.

However, this is not unreasonable. In other words, this is not a problem, thus it does not need to be resolved. There is no ground-truth relationship between $\text{sim}_{BC}(G1, G2)$ and $\text{sim}_{BC}(G1, G3)$. The reason is described below.

When measuring the similarity between two vectors, there are two factors to be considered: 1. the sizes of the vectors (i.e. the distance between the two vectors), 2. the directions of the vectors (i.e. the angle between the two vectors). In this context of measuring similarity between tissue-wide expression values of genes (each gene is mapped to a vector), both factors matter.

It is stated in the Methods section that Bray-Curtis Similarity satisfies three desirable properties. In fact, Property 2 (achieving the maximal similarity value 1 if and only if two vectors are identical) ensures Factor 1 to be considered, and Property 3 (larger values having a larger impact on the resultant similarity value) ensures Factor 2 to be considered.

Thus, Table 1 shows that Bray-Curtis Similarity is more appropriate than the other five metrics, which is exactly due to the fact it takes both factors into account. In contrast, Euclidean Similarity does not take vectors' directions into account; Cosine Similarity, Pearson Correlation and Spearman Correlation do not take the sizes of the vectors into account.

Thus, to be able to infer a ground-truth similarity relationship, on both Factor 1 and Factor 2 the intuitive comparison results must be concordant. In Example 1 (see Additional File 1), the angle between Gene A and Gene C is identical to that between Gene B and Gene C, and the distance between A and C is larger than that between B and C; thus, $\text{sim}(A, C) < \text{sim}(B, C)$. Similarly, the distance between A and D is identical to that between E and F, and the angle between A and D is larger than that between E and F; thus, $\text{sim}(A, D) < \text{sim}(E, F)$.

But in this case, the distance between Gene 1 and Gene 2, i.e. $9 \cdot \sqrt{a^2 + b^2}$, is larger than that between Gene 1 and Gene 3, i.e. $(b-a)/\sqrt{2}$, but the angle between Gene 1 and Gene 2 (i.e. 0) is smaller than that between Gene 1 and Gene 3 (> 0). Thus, a ground-truth similarity relationship is unable to be inferred.

Thus, the result given by Bray-Curtis Similarity, i.e. $\text{sim}_{BC}(G1, G3) > \text{sim}_{BC}(G1, G2)$, is not unreasonable.

Comment 3: Every time a machine learning method is named, it should be clear: (1) what are the input features (ii) what are the labels -- i.e. what is being classified (iii) what is the cross-validation or training-testing-validation scheme. Since there are so many machine learning things being done, it is hard sometimes to make sense of what is being done in each specific case.

Response: In the module to predict genes with similar tissue-wide expression profiles to a particular gene, to make these points clearer, the following changes were made:

(i) Using the red color Figure 1A shows that seven features were derived from TFBS clusters. In addition, in the legend of Figure 1A, the following sentence was added “The seven ML features derived from TFBS clusters were described in the Methods section.” The second paragraph of the second subsection of the Methods section details the seven features; its first sentence was revised to “The seven information density-related ML features derived from each TFBS cluster included ...”

(ii) The first sentence of the ‘Prediction of genes with similar tissue-wide expression profiles’ subsection of the Methods section was revised to ‘The framework for predicting whether the tissue-wide expression profile of a gene resembles a particular gene is indicated in Figure 1A, B.’, so that it is clear that the two labels are ‘similar to the particular gene’ and ‘dissimilar to the particular gene’. In addition, Figure 1B also indicates that 500 most similar genes and 500 most dissimilar genes were selected as positives and negatives.

(iii) The last step (‘Performance evaluation’) of Figure 1A was revised to ‘Performance evaluation (ROC curve/10-fold cross validation)’; the red color indicates that ROC curves were used to validate the classifiers in this module. In addition, the last sentence of the legend of Figure 1A was revised to “The performance of ML classifiers was evaluated with ROC curves and 10-fold cross validation”.

The last sentence of the second subsection of the Methods section was revised to “This allowed all genes to be used as training data for ML classifiers. Default parameter values for these classifiers were used to generate ROC curves in MATLAB”, and also the first sentence of the corresponding second subsection of the Results section was revised to “Several ML classifiers (Naïve Bayes, Decision Tree (DT), Random Forest and Support Vector Machines (SVM) with four different kernels) were evaluated to determine how well TFBS-related features could predict genes with tissue-wide expression profiles similar to NR3C1. Their performance were compared using ROC curves...”. Thus, it is now clear that ROC curves were used to validate the classifiers and all instances were used as training data (i.e. there were no test sets).

In the module to predict TF target genes, to make these points clearer, the following changes were made:

(i) Using the blue color Figure 1A shows that six features were derived from TFBS clusters. Also, the penultimate sentence of the last paragraph of the “Using gene expression in the CRISPR-based perturbations” subsection of the Methods section states “Six features (Features 1-5 and 7) were derived from each homotypic cluster (i.e. Feature 6 became identical to Feature 3, because only binding sites from a single TF were used) (Figure 1A)”. Combining with the detailed descriptions about what the features are in the second paragraph of the previous subsection, it is clear that these six features (Features 1-5 and 7) were used.

(ii) The last sentence of the first paragraph of the ‘Using gene expression in the CRISPR-based perturbations’ subsection of the Methods section was revised to “We defined a positive TF target gene in a cell line as:...”. And the sentence in the fifth paragraph was revised to “If the coefficients of all guide RNAs of the TF for a gene are zero, the gene was defined as a negative (i.e. a non-target gene).” Thus it is clear that the two labels are “TF target genes” and “non-target genes”. Combining with the last sentence of the first paragraph of the Methods section, ‘Since

protein-coding (PC) sequences represent the most widely studied and best understood component of the human genome [19], positives and negatives for deriving machine learning classifiers for predicting DE direct TF target genes that encode proteins (TF targets, below) were obtained from CRISPR- and siRNA-generated knockdown data', it is clear that the 'target genes' here stands for 'PC, direct, DE target genes'.

(iii) As stated above, the last step ('Performance evaluation') of Figure 1A was revised to 'Performance evaluation (ROC curve/10-fold cross validation)'; the blue color indicates that 10-fold cross validations were used to validate the classifiers in this module. In addition, the last sentence of the legend of Figure 1A was revised to "The performance of ML classifiers was evaluated with ROC curves and 10-fold cross validation". The last sentence of the last paragraph of the "Using gene expression in the CRISPR-based perturbations" subsection of the Methods section was revised to "The results of 10 rounds of 10-fold cross validation were averaged to evaluate the accuracy of the classifier." Thus it is clear that the validation scheme is 10-fold cross validation.

Comment 4: For the method described in (B) in Fig 1: Does it necessarily make sense to compare the 'most similar' to the 'least similar'? Genes that have exactly the opposite gene expression pattern to the one you are interested might be tightly regulated by a different set of TFs. You might be picking up this signal instead of the one you care about! This might be an even bigger issue since you are using raw gene expression values-- genes that are very highly or very lowly expressed in all tissues might always come up in your negative set.:

Response: Yes, it makes sense. As stated in the above response to Comment 3, in this module to predict genes with similar tissue-wide expression profiles to a particular gene, the two labels are 'similar to the given gene' and 'dissimilar to the given gene'. Therefore, it makes the most sense that the most similar genes were selected as positives and the most dissimilar genes were selected as negatives.

The first sentence of the last paragraph of the Background section, "...the distribution and composition of *cis*-regulatory modules in promoters substantially determines gene expression profiles..., is exactly the underlying rationale why this machine learning framework is able to distinguish between "similar genes" and "dissimilar genes". In other words, "similar genes" and "dissimilar genes" have different expression patterns, presumably because they have different organizations and compositions (i.e. different TF sets) of TFBSs in their promoters. Therefore, the potential fact that "similar genes" and "dissimilar genes" are regulated by different TF sets was exactly what we expected to see and validate.

Comment 5: Biologists don't just want good classifiers, they want feature selection! Can you show the Gini scores of the features in a supplemental table?:

Response: In the module to predict TF target genes based on CRISPR- and siRNA-generated knockdown data, to assess the relative importance of the six features to the Decision Tree classifiers, we computed their Gini importance values, which are added to Additional file 5.

For the seven CRISPR-perturbed TFs in the K562 cell line, the cluster-level Features 1-3, especially Feature 3 capturing the information density of TFBS clusters, have the largest contribution to the classifiers' predictive power. By contrast, for the 11 siRNA-perturbed TFs in the GM19238 cell line, the binding site-level Feature 5 capturing the spatial distribution of strong TFBSs has the largest contribution.

Accordingly, in this revision, this observation is described in the second and third sentences of the first paragraph of the third subsection of the Results section.

Comment 6: Is all the code for generating every figure available online? Let's help make research reproducible.

Response: As stated in the Software availability section, the code that implemented this machine learning framework and produced all the results has been deposited at <https://bitbucket.org/cytognomix/information-dense-transcription-factor-binding-site-clusters/src> and <https://doi.org/10.5281/zenodo.1892051>. The input of the code to derive the figures is directly taken from the output of the ML framework code. There are no intermediate steps or variable required to generate the figures in MATLAB.

The code for generating the figures is used to visualize the results. In this revision, we also deposited the MATLAB code for generating all the figures at <https://bitbucket.org/cytognomix/information-dense-transcription-factor-binding-site-clusters/src>

Comment 7: If you have 10 values (from cross validation), why don't you show them all in Figure 4 so we can evaluate the spread.

Response: To avoid making Figure 4 too complicated, in this revision, the accuracy values of all individual rounds of 10-fold cross validations in prediction of TF target genes were added to Additional file 5. Accordingly, the legends of Table 2, Figure 4 and Table 3 were revised to indicate this.

Comment 8: "Our in-silico mutation analyses revealed that some deleterious TFBS mutations could be compensated for by other information-dense clusters in the same promoter(2); thus, predicting the effects of mutations in individual binding sites might not be sufficient to interpret downstream effects without considering their context." This is something that me and my collaborators have recently studied³. Don't feel pressure to add this citation-- I just thought it would be interesting for you to read! (Also, thanks for discussing IDBC in this paper-- I hadn't heard of it before but it would be relevant to my research.)

Response: In this revision, this publication has now been referenced (number 47) in the manuscript.

Comment 9: It would be great if you discussed how Bray-Curtis is used in other fields in the Discussion.

Response: The following sentences were added to the penultimate paragraph, "Previous applications of this index include: a) measurement of the ecological transfer of species abundance from dense to sparse plots⁴⁸ and comparative difference analyses of species quantities between reference and algorithm-derived metagenomic sample mixtures (<https://precision.fda.gov/challenges/3/view/results>). b) improvement of friend recommendation in geosocial networks by using it to compare users' movement history^{49, 50} .."

Comment 10: Better subsection names in the results section - emphasizing the biological conclusions rather than what was done.

Response: In the Results section of this revision, the title of each subsection was revised as follows, now summarizing the primary conclusion from this subsection.

The title of the first subsection was revised from 'Similarity between GTEx tissue-wide expression profiles of genes' to 'The Bray-Curtis Function can accurately quantify the similarity between tissue-wide gene expression profiles'.

The title of the second subsection was revised from 'Prediction of genes with similar GTEx tissue-wide expression profiles' to 'The Decision Tree classifier performed best in prediction of genes with similar tissue-wide expression profiles'.

The title of the third subsection was revised from 'Prediction of TF targets' to 'The Decision Tree classifier was predictive of TF target genes'.

The title of the fourth subsection was revised from 'Intersection of genes with similar tissue-wide expression profiles and TF targets' to 'Some TF target genes also display similar tissue-wide expression profiles to the TFs, themselves'.

The title of the fifth subsection was revised from 'Mutation analyses on promoters of direct targets' to 'Transcription factor binding site clusters buffer against expression changes from mutations in single sites'.

Competing Interests: none

The benefits of publishing with F1000Research:

- Your article is published within days, with no editorial bias
- You can publish traditional articles, null/negative results, case reports, data notes and more
- The peer review process is transparent and collaborative
- Your article is indexed in PubMed after passing peer review
- Dedicated customer support at every stage

For pre-submission enquiries, contact research@f1000.com

F1000Research